

Characterization of a zebrafish *tbk1* model of  
Amyotrophic Lateral Sclerosis

Olivia G. Persia

Integrated Program in Neuroscience

McGill University

Montreal Neurological Institute

June 2024

A thesis submitted to McGill University in partial fulfillment of the requirements  
of the degree of *Master of Science*

© Olivia G. Persia 2024

Supervisor: Dr. Gary Armstrong

Advisory Committee:

Dr. Benoit Gentil and Dr. Jo Anne Stratton

## **Table of Contents**

Abstract.....	3
Acknowledgments.....	8
Contribution of Authors .....	11
List of Figures and Tables .....	12
List of Abbreviations .....	13
Introduction: Rationale, Aims, and Hypotheses.....	16
1. Background Knowledge and Review of Relevant Literature.....	19
1.1 Amyotrophic Lateral Sclerosis.....	19
1.2 TANK-Binding Kinase 1 (TBK1) .....	27
1.3 Animal Models of TBK1.....	34
2. Materials and Methods .....	37
3. Results.....	48
4. Discussion.....	68
5. Conclusion.....	79
6. Bibliography .....	81

## Abstract

Amyotrophic Lateral Sclerosis (ALS) is a devastating neurodegenerative disease characterized by the progressive degeneration of motor neurons, leading to muscle paralysis and, ultimately, death within 2-5 years of diagnosis for most patients. Despite intensive research efforts, effective therapies for ALS remain elusive, emphasizing the need for innovative approaches to understand its underlying mechanisms and develop treatments. Recent studies have identified heterozygous mutations in the TANK-Binding Kinase 1 (*TBK1*) gene in both familial and sporadic cases of ALS. TBK1 is a multifunctional kinase with pivotal roles in innate immune response, selective autophagy, mitophagy, and apoptosis by inducing the expression of type I/III interferons. Understanding the functional role of TBK1 in the development of ALS is of crucial interest due to the close association of TBK1 with autophagy and neuroinflammation, two cellular mechanisms known to be dysregulated in ALS patients. In this thesis, I present an initial characterization of a zebrafish *tbk1* knockout model generated using the CRISPR/Cas9 genome editing system to elucidate the role of TBK1 in ALS. Zebrafish provide an advantageous model due to their genetic manipulability and conservation of disease-related pathways. It was hypothesized that *Tbk1*-deficient zebrafish would exhibit ALS-like phenotypes, including motor dysfunction and neuroinflammation. A nonsense mutation causing multiple premature stop codons in the eleventh exon of the zebrafish *tbk1* gene resulted in a transcript likely degraded via nonsense-mediated decay, analogous to patient observations. Notably, homozygous knockout zebrafish larvae failed to survive beyond 15 days post-fertilization (dpf), displaying hyperactive swimming behavior at 2 dpf, followed by impaired motor activity at 8 dpf, preceding their death. Immunofluorescence analysis of neuromuscular junctions (NMJs) at 2 dpf revealed that homozygous KO (*tbk1*<sup>-/-</sup>) larvae exhibited increased orphaned pre- and post-synaptic markers

compared to wild-type (WT) and heterozygous KO (*tbk1*<sup>+/-</sup>) larvae, suggesting synaptic defects. Furthermore, adult *tbk1*<sup>+/-</sup> zebrafish do not exhibit discernible motor phenotype at 1.5 years of age. In adult *tbk1*<sup>+/-</sup> zebrafish, upregulated expression of *irf3*, *irf7*, and *p62*, and downregulated expression of *optn*, *il8*, *il10*, and *ripk1* transcripts were observed, indicating a potential dysregulation of immune response and autophagy due to haploinsufficiency. To evaluate the transcriptional impact of *tbk1* following an immune challenge, both WT and WT x *tbk1*<sup>+/-</sup> larvae were exposed to lipopolysaccharide (LPS)-treated system water. Notably, LPS exposure did not alter *tbk1* transcript levels when compared to WT larvae. However, transcriptional changes included upregulation of *p62* and *il6*, and downregulation of *il8* and *ndp52* in the WT x *tbk1*<sup>+/-</sup> offspring. Comparative analysis of adult brain and larval expression data revealed that downregulation of *il8* and upregulation of *p62* are consistent consequences of heterozygous *tbk1* loss across developmental stages. Furthermore, elevated expression of *tnfa* and *nfkb1* was observed in response to LPS in both WT and WT x *tbk1*<sup>+/-</sup> larvae, while *il6* expression was reduced in the WT x *tbk1*<sup>+/-</sup> larvae under similar conditions. These findings highlight the interplay between TBK1 signaling and the regulation of key inflammatory mediators in zebrafish under immune stress. Overall, this research advances our understanding of ALS pathogenesis through a zebrafish model, offering critical insights into TBK1's involvement in immune and autophagy dysregulation. This foundational work not only enhances our knowledge of TBK1's involvement in ALS but also paves the way for future studies aimed at identifying therapeutic targets for this devastating disease.

## Résumé

La sclérose latérale amyotrophique. (SLA) est une maladie neurodégénérative dévastatrice caractérisée par la dégénérescence progressive des motoneurones, entraînant une paralysie musculaire et, finalement, la mort dans les 2 à 5 ans suivant le diagnostic pour la plupart des patients. Malgré des efforts de recherche intensifs, les thérapies efficaces contre la SLA restent insaisissables, soulignant la nécessité d'approches innovantes pour comprendre ses mécanismes sous-jacents et développer des traitements. Des études récentes ont identifié des mutations hétérozygotes dans le gène de la kinase 1 liée à TANK (*TBK1*) dans des cas familiaux et sporadiques de SLA. TBK1 est une kinase multifonctionnelle ayant des rôles cruciaux dans la réponse immunitaire innée, l'autophagie sélective, la mitophagie et l'apoptose en induisant l'expression des interférons de type I/III. Comprendre le rôle fonctionnel de TBK1 dans le développement de la SLA est d'un intérêt crucial en raison de l'association étroite de TBK1 avec l'autophagie et la neuroinflammation, deux mécanismes cellulaires connus pour être dysrégulés chez les patients atteints de SLA. Dans cette thèse, je présente une caractérisation initiale d'un modèle knockout de *tbk1* chez le poisson-zèbre généré en utilisant le système d'édition du génome CRISPR/Cas9 pour élucider le rôle de TBK1 dans la SLA. Les poissons-zèbres offrent un modèle avantageux en raison de leur manipulabilité génétique et de la conservation des voies liées à la maladie. Il a été émis l'hypothèse que les poissons-zèbres déficients en *Tbk1* présenteraient des phénotypes similaires à ceux de la SLA, y compris une dysfonction motrice et une neuroinflammation. Une mutation non-sens entraînant plusieurs codons d'arrêt prématurés dans le onzième exon du gène *tbk1* du poisson-zèbre a abouti à une transcription probablement dégradée via la dégradation médiée par non-sens, analogue aux observations chez les patients. Notamment, les larves knockout homozygotes n'ont pas survécu au-delà de 15 jours post-

fertilisation (jpf), présentant un comportement de nage hyperactif à 2 jpf, suivi d'une activité motrice altérée à 8 jpf, précédant leur mort. L'analyse par immunofluorescence des jonctions neuromusculaires (JNM) à 2 jpf a révélé que les larves *tbk1*<sup>-/-</sup> présentaient des marqueurs pré- et post-synaptiques orphelins augmentés par rapport aux larves de type sauvage WT et *tbk1*<sup>+/-</sup>, suggérant des défauts synaptiques. De plus, les poissons-zèbres adultes *tbk1*<sup>+/-</sup> ne présentent pas de phénotype moteur discernable à l'âge de 1,5 ans. Chez les poissons-zèbres adultes *tbk1*<sup>+/-</sup>, une expression accrue de *irf3*, *irf7* et *p62*, et une expression réduite de *optn*, *il8*, *il10* et *ripk1* ont été observées, indiquant une potentielle dysrégulation de la réponse immunitaire et de l'autophagie due à une haplo-insuffisance. Pour évaluer l'impact transcriptionnel de *tbk1* suite à un défi immunitaire, des larves WT et WT x *tbk1*<sup>+/-</sup> ont été exposées à de l'eau traitée au lipopolysaccharide (LPS). Notamment, l'exposition au LPS n'a pas altéré les niveaux de transcription de *tbk1* par rapport aux larves WT. Cependant, les changements transcriptionnels incluaient une régulation à la hausse de *p62* et *il6*, et une régulation à la baisse de *il8* et *ndp52* chez les descendants WT x *tbk1*<sup>+/-</sup>. L'analyse comparative des données d'expression cérébrale adulte et larvaire a révélé que la régulation à la baisse de *il8* et la régulation à la hausse de *p62* sont des conséquences constantes de la perte hétérozygote de *tbk1* à travers les stades de développement. De plus, une expression accrue de *tnfa* et *nfkb1* a été observée en réponse au LPS chez les larves WT et WT x *tbk1*<sup>+/-</sup>, tandis que l'expression de *il6* était réduite chez les larves WT x *tbk1*<sup>+/-</sup> dans des conditions similaires. Ces résultats mettent en évidence l'interaction entre la signalisation TBK1 et la régulation des médiateurs inflammatoires clés chez le poisson-zèbre sous stress immunitaire. Dans l'ensemble, cette recherche fait progresser notre compréhension de la pathogenèse de la SLA à travers un modèle de poisson-zèbre, offrant des aperçus critiques sur l'implication de TBK1 dans la dysrégulation de l'immunité et de l'autophagie. Ce travail

fondamental non seulement enrichit notre connaissance de l'implication de TBK1 dans la SLA mais ouvre également la voie à de futures études visant à identifier des cibles thérapeutiques pour cette maladie dévastatrice.

## **Acknowledgments**

I am profoundly grateful to the members of the Armstrong lab for their unwavering support and encouragement throughout my master's program. First and foremost, I would like to thank Dr. Gary Armstrong, whose exceptional mentorship and guidance have been pivotal in my academic journey. His deep passion for science, combined with his enthusiasm for our discoveries, has been a continuous source of inspiration and motivation for me. His ability to ignite excitement and curiosity in his students is truly remarkable. I extend my heartfelt thanks to Ziyaan, Christian, and Tyler for their invaluable assistance with training and troubleshooting during my experiments. Their technical expertise and willingness to help have been instrumental in the success of my research. Beyond their professional support, their camaraderie and friendship have made my time in the lab enjoyable and fulfilling. From late-night discussions about experimental results to shared celebrations of our successes, their presence has made a significant impact on my experience, and I am honored to know our friendships will last a lifetime. A special note of appreciation goes to Virginie, whose vast knowledge and experience have been an incredible resource for me. I am deeply thankful to Esteban, our lab manager and research assistant, for his exceptional dedication and meticulous attention to detail. His organizational skills and work ethic are the backbone of our lab's operations, ensuring that everything runs smoothly. Esteban's innovation and unwavering commitment to maintaining high standards have been crucial to our lab's success. I consider myself incredibly fortunate to be part of this exceptional group of individuals. The collaborative spirit and supportive environment fostered by Dr. Armstrong and my colleagues have not only advanced our research but also created a sense of belonging and mutual respect. I am confident that this research group will continue to excel and produce high-quality data under Dr. Armstrong's visionary leadership.

I would also like to express my gratitude to the other research groups on the sixth floor of the Montreal Neurological Institute and Hospital. Their friendship and shared scientific curiosity have created an environment where we continually push each other toward groundbreaking discoveries. The collaborative atmosphere and intellectual exchanges have enriched my research experience and broadened my scientific horizons. My deepest appreciation goes to my advisory committee, Dr. Benoit Gentil and Dr. Jo Anne Stratton, and mentor, Dr. Michel Cayouette, whose insightful feedback and guidance have been invaluable throughout my project. Their expertise and thoughtful critiques have helped refine my research and have significantly contributed to my academic growth. My time at McGill University, particularly at the Montreal Neurological Institute, has been profoundly rewarding. The vibrant academic environment and the opportunity to work with some of the brightest minds in neuroscience have been a dream come true.

To my parents, Dr. Albert Persia and Sabena Steenburg-Persia, thank you for your unwavering love and support. Your dedication to your careers and your emphasis on the importance of education has been a constant source of inspiration. Your guidance, encouragement, and belief in my abilities have been the foundation of my achievements. I strive to honor the values you've instilled in me throughout the course of my life. Thank you to my younger brother, Matthew Persia, for being an extraordinary individual. Watching you grow and develop into the person you are today has been one of the greatest joys of my life. Sharing my passions with you and witnessing your own interests and talents blossom has been incredibly fulfilling. To my extended family—grandparents, aunts, uncles, and cousins—your unwavering support and genuine interest in my pursuits have meant the world to me. Your encouragement has provided a strong foundation for my academic and personal growth. Finally, to my dear friends, whether we have known each other since childhood or met more recently, whether you

are in Montreal, Lakewood, or elsewhere around the globe, thank you for always supporting and encouraging me to follow my dreams. Your friendship has been a source of strength and joy, and I cherish the moments we have shared.

I would like to thank everyone mentioned in these acknowledgments for shaping me into the person I am today. As I transition to medical school, I carry with me a wealth of knowledge, skills, and experiences gained through this journey. I embark on this next chapter with a solid foundation of scientific knowledge, practical skills, and a deep appreciation for the human elements of medicine. I am excited to integrate these experiences into my medical education, aiming to become a compassionate, knowledgeable, and innovative physician. Thank you all for your invaluable contributions to my journey.

## **Author Contributions**

Olivia Persia was the primary researcher for this study. She was responsible for the planning, execution, and analysis of the experiments, working under the close supervision of Dr. Gary Armstrong. Throughout the project, she received invaluable guidance and support from her advisory committee members, Dr. Benoit Gentil and Dr. Jo Anne Stratton. Olivia Persia was the principal author of this thesis, drafting the initial and subsequent versions. Dr. Gary Armstrong meticulously reviewed and provided critical feedback on the manuscript, ensuring its academic rigor and coherence. The *in vitro* fertilization experiments were expertly conducted by Esteban Rodriguez Pinto. His technical expertise and dedication significantly contributed to the success of these experiments. Further assistance and specialized training on experimental protocols were generously provided by Ziyaan Harji, Christian Rampal, Tyler Gurberg, and Dr. Gary Armstrong. Their collective efforts in training and knowledge transfer were essential for the development and refinement of the experimental techniques employed in this study. Together, these contributions were pivotal in advancing the research objectives and ensuring the overall success of the thesis.

## **List of Figures and Tables**

Figure 1 | Schematic of human TBK1 primary structure

Figure 2 | Schematic representation of TBK1's functional role in inflammation

Figure 3 | Human TBK1 vs. zebrafish Tbk1 amino acid sequence comparison

Figure 4 | Generation of a zebrafish *tbk1* KO line

Figure 5 | RT-qPCR analysis of adult and larval *tbk1* expression

Figure 6 | Genotypic frequency of WT, *tbk1*<sup>+/-</sup>, and *tbk1*<sup>-/-</sup> zebrafish larvae at 2, 5, 10, and 15 dpf

Figure 7 | 2 dpf touch-evoked motor response assay

Figure 8 | 8 dpf DanioVision motor response assay

Figure 9 | Neuromuscular junction abnormalities

Figure 10 | Adult swim tunnel and free swim motor function assays

Figure 11 | RT-qPCR analysis of Tbk1-associated inflammatory markers in adult zebrafish

Figure 12 | RT-qPCR analysis under LPS stimulation in zebrafish larvae

## Abbreviation list

<b>Abbreviation</b>	<b>Meaning</b>
°C	degree Celsius
aBtx	alpha-bungarotoxin
ALS	amyotrophic lateral sclerosis
ALSFRS-R	revised ALS functional rating scale
C9ORF72	chromosome 9 open reading frame 72
cDNA	complementary DNA
CRISPR	clustered regularly interspaced short palindromic repeats
DNA	deoxyribonucleic acid
dpf	days post fertilization
EF1 $\alpha$	Eukaryotic elongation factor 1 alpha
fALS	familial amyotrophic lateral sclerosis
FTD	frontotemporal dementia/degeneration
FUS	Fused in sarcoma
GAPDH	Glyceraldehyde-3-phosphate dehydrogenase
gRNA	guide ribonucleic acid
HRM	high resolution melting
IFN	interferon
IL-1 $\beta$	Interleukin 1beta
IL-6	Interleukin 6
IL-8	Interleukin 8

IL-10	Interleukin 10
IRF3	Interferon regulatory factor 3
IRF7	Interferon regulatory factor 7
kDa	kilodalton
KO	knockout
LOF	loss-of-function
mg	milligram
mL	millilitre
MNI	Montreal Neurological Institute
mRNA	messenger ribonucleic acid
NBR1	Neighbor of BRCA1 gene 1
NDP52	Nuclear dot protein 52 kDa
NF- $\kappa$ B	Nuclear factor kappa-light-chain-enhancer of activated B cells
ng	nanogram
nL	nanolitre
NMJ	neuromuscular junction
OPTN	Optineurin
P62/ SQSTM1	P62/ Sequestome 1
PCR	polymerase chain reaction
PBS	phosphate-buffered saline
PFA	paraformaldehyde
RIPK1	Receptor-interacting protein kinase 1

RT-qPCR	quantitative real-time PCR
RNA	ribonucleic acid
ROS	reactive oxygen species
RT	room temperature
sALS	sporadic amyotrophic lateral sclerosis
SOD1	Superoxide dismutase 1
TBK1	TANK-binding kinase 1
TDP-43/ TARDBP	TAR DNA-binding protein 43
TNF $\alpha$	Tumor necrosis factor alpha
$\mu$ g	microgram
$\mu$ L	microlitre
WT	wild type

## **Introduction: Rationale, Aims, and Hypotheses**

ALS is a fatal neurodegenerative disease characterized by the progressive degeneration of the upper and lower motor neurons (Kiernan et al., 2011). There is no cure and few treatment options, with current therapies only offering modest benefits for the 1,000 Canadians diagnosed every year. Recent studies have identified heterozygous mutations in the TANK-Binding Kinase 1 (*TBK1*) gene in both familial and sporadic cases of ALS (Cirulli et al., 2015; Freischmidt et al., 2015). TBK1 is a ubiquitously expressed serine/threonine protein kinase with a critical role in innate immune response, selective autophagy, mitophagy, and apoptosis (Oakes, Davies, & Collins, 2017). Despite its importance, there is a notable lack of animal models that accurately mimic TBK1 dysfunction, hindering the study of ALS-related mutations. This thesis aimed to address this gap by developing and characterizing a *tbk1* knockout zebrafish model to assess the impact of Tbk1 deficiency on motor function, neuromuscular junction integrity, and immune responses in zebrafish larvae and adult fish. Zebrafish are an excellent vertebrate model for studying TBK1-related ALS due to their substantial homology with the human TBK1 protein and anatomical and neurochemical similarities between their central nervous systems (Howe et al., 2013). While mouse models of Tbk1 loss-of-function have been described (Bonnard et al., 2000; Brenner et al., 2019), the development of novel animal models remains crucial for advancing our understanding of neurodegeneration and therapeutic development. In this thesis, I present research that elucidates the role of Tbk1 in neuroinflammatory processes and the pathogenesis of ALS-like phenotypes, potentially informing future therapeutic strategies targeting TBK1 and immune dysregulation in ALS.

### **Aim 1: Generation of a CRISPR knockout line (KO) of zebrafish *tbk1*.**

The zebrafish genome contains an orthologous *tbk1* gene located on chromosome 12. TBK1's role in regulating innate immune responses and autophagy makes it a promising target for studying neurodegenerative diseases such as ALS. To model a mutation analogous to one observed in an ALS patient from the Montreal Neurological Institute, I utilized the CRISPR/Cas9 gene-editing system to introduce a single nucleotide deletion in exon 11. This deletion, which encodes part of the coiled-coil domain 1, results in several premature stop codons that likely result in the transcript being sent for nonsense-mediated decay.

### **Aim 2: Assessment of motor function in larval and adult *Tbk1* deficient (*tbk1*<sup>+/-</sup> and *tbk1*<sup>-/-</sup>) zebrafish.**

Zebrafish are advantageous for studying motor function and dysfunction due to the conservation of key developmental and physiological processes across vertebrates (Babin, Goizet, & Raldua, 2014). Using homozygous (*tbk1*<sup>-/-</sup>) and heterozygous (*tbk1*<sup>+/-</sup>) KO models, motor phenotypes in both larval and adult zebrafish were assessed, including locomotor activity and synaptic components of the neuromuscular junctions (NMJs). Additionally, I examined the Mendelian ratio adherence of *tbk1* knockout fish to understand their viability during development. I hypothesized that *tbk1*<sup>-/-</sup> knockout zebrafish will not survive to sexual maturity and will exhibit reduced motor function compared to wild-type counterparts. Furthermore, I anticipate that *tbk1*<sup>+/-</sup> zebrafish will also demonstrate reduced motor function in both larval and adult stages.

**Aim 3: Investigation of transcriptional changes in inflammatory cellular pathways associated with Tbk1 signaling in *tbk1* mutant zebrafish.**

Zebrafish possess a repertoire of cytokines involved in neuroinflammation, similar to those found in humans (Xie, Meijer, & Schaaf, 2020), making them a suitable model for investigating inflammatory mechanisms underlying neurodegenerative disorders.

Lipopolysaccharides (LPS), essential outer membrane glycolipids of gram-negative bacteria, trigger potent immune responses (Power, Peng, Maydanski, Marshall, & Lin, 2004). Zebrafish can mount an inflammatory response to LPS as early as 2 days post-fertilization (Novoa, Bowman, Zon, & Figueras, 2009). Using my *tbk1* knockout models, I examined the expression levels of inflammatory markers associated with TBK1-ALS pathology to evaluate their immune response to LPS treatment. Understanding the immune response in the context of an orthologous ALS-associated mutation is crucial for elucidating the role of inflammation in disease progression. I hypothesized reduced expression of inflammatory markers in *tbk1*-deficient zebrafish and an aberrant immune response to LPS compared to their WT siblings, underscoring the regulatory role of Tbk1 in inflammatory pathways implicated in ALS.

## **1. Background Knowledge and Review of Relevant Literature**

### **1.1 Amyotrophic Lateral Sclerosis**

#### **1.1.1 Brief Description, History, and Etymology of Amyotrophic Lateral Sclerosis**

Amyotrophic lateral sclerosis (ALS), commonly known in the United States as Lou Gehrig's disease and referred to as motor neuron disease (MND) in Europe, is a debilitating and fatal neurodegenerative disease. It is characterized by the selective vulnerability and progressive degeneration of both upper motor neurons in the cerebral cortex and lower motor neurons in the brainstem and spinal cord. This degeneration leads to a cascade of neuromuscular symptoms, including muscle weakness, atrophy, and spasticity, ultimately resulting in paralysis and subsequent death (Hardiman et al., 2017; Kiernan et al., 2011).

The initial description of ALS dates back to 1869 when French neurologist Jean-Martin Charcot provided a comprehensive clinical and pathological characterization of the condition (Masrori & Van Damme, 2020). The term "amyotrophic lateral sclerosis" was coined by Charcot, encapsulating the disease's core pathological features. The etymology of "amyotrophic" is rooted in Greek: 'a' meaning no or negative, 'myo' referring to muscle, and 'trophic' meaning nourishment, thus translating to "no muscle nourishment," which succinctly captures the muscle wasting observed in ALS patients. "Lateral sclerosis" refers to the hardening (sclerosis) of the lateral corticospinal tracts in the spinal cord as upper motor neurons degenerate and are replaced by gliosis, a type of scarring (Masrori & Van Damme, 2020; Rowland, 2001).

The early 20th century marked significant milestones in the awareness and understanding of ALS. In 1939, the diagnosis of ALS in the iconic American baseball player Lou Gehrig brought unprecedented public attention to the disease. Gehrig's emotional farewell speech and

subsequent death in 1941 heightened public awareness and empathy towards ALS, leading to its alternative name, "Lou Gehrig's disease."

### 1.1.2 Aetiology and Pathophysiology of ALS

The aetiology of ALS is multifactorial, involving a complex interplay of environmental, genetic, and molecular factors that are not yet fully understood (Peters, Ghasemi, & Brown, 2015). Epidemiologically, ALS has an annual incidence rate of approximately 1-2 cases per 100,000 individuals, with a slightly higher prevalence in males compared to females (Kiernan et al., 2011; Talbott, Malek, & Lacomis, 2016). The median age of onset for this disease is between 50 to 65 years of age (Zarei et al., 2015), depending on the geographical location and wealth of the sub-population of interest (Longinetti & Fang, 2019; L. Xu et al., 2020; Zarei et al., 2015). The environmental risk factors associated with a higher risk of triggering ALS include diet, smoking, and exposure to metals or pesticides (Q. Q. Duan et al., 2023; Oskarsson, Horton, & Mitsumoto, 2015). The risk of this disease was also shown to be associated with health conditions related to viruses, metabolic alterations, or innate immune dysregulation (Ingre, Roos, Piehl, Kamel, & Fang, 2015; Oskarsson et al., 2015).

Approximately 5-10% of ALS cases are familial (fALS), linked to inherited genetic mutations, whereas the remaining cases are sporadic (sALS), with no clear familial component (Kiernan et al., 2011; Masrori & Van Damme, 2020). Over 40 genes have been implicated in ALS pathogenesis, illustrating the genetic heterogeneity of the disease (Cirulli et al., 2015). Approximately 70% of fALS cases are associated with four of the identified genes: chromosome 9 open reading frame 72 (*C9ORF72*), Superoxide dismutase 1 (*SOD1*), Transactive response

DNA-binding protein (*TARDBP*), and Fused in sarcoma (*FUS*) (Masrori & Van Damme, 2020; Ragagnin, Shadfar, Vidal, Jamali, & Atkin, 2019).

Among the genetic factors, a hexanucleotide repeat expansion of the "GGGGCC" sequence in the *C9ORF72* gene is the most prevalent, accounting for 30-50% of fALS and 7-10% of sALS cases among individuals of European descent (DeJesus-Hernandez et al., 2011; Renton et al., 2011). This mutation leads to reduced expression of the *C9ORF72* protein, which is involved in autophagy and inflammatory response regulation (Smeyers, Banchi, & Latouche, 2021).

The first gene associated with ALS was *SOD1*, identified in 1993. Mutations in *SOD1* are implicated in approximately 20% of fALS and 5% of sALS cases (Rosen et al., 1993). These mutations often result in a toxic gain-of-function mechanism, where the altered *SOD1* protein aggregates and loses its capacity to mitigate reactive oxygen species (ROS), thereby contributing to oxidative stress and motor neuron death (Masrori & Van Damme, 2020; Rosen et al., 1993)

In addition to *C9ORF72* and *SOD1*, significant genetic contributors to ALS include *TARDBP* (TDP-43) and *FUS*. Missense mutations in these genes are thought to cause their associated protein variants to mislocalize and aggregate in the cytoplasm. Protein aggregation disrupts cellular homeostasis, impairing protein degradation pathways and triggering cellular stress responses, collectively exacerbating neuronal impairment. Mutations in *TARDBP* and *FUS* are responsible for 3-5% of fALS and about 1-2% of sALS cases (Kwiatkowski et al., 2009; Masrori & Van Damme, 2020; Rutherford et al., 2008; Vance et al., 2009). Although *TARDBP* mutations account for around 5% of all ALS cases, it is estimated that nearly 97% of ALS cases, and up to 45% of frontotemporal dementia (FTD) cases, present with cytoplasmic

mislocalization of TDP-43 (Ling, Polymenidou, & Cleveland, 2013; Scotter, Chen, & Shaw, 2015)

In addition to protein aggregation, several cellular pathways are implicated in the development of pathology. Protein aggregation is a hallmark of ALS, often occurring alongside autophagic impairment (Blokhuys, Groen, Koppers, van den Berg, & Pasterkamp, 2013; Iguchi et al., 2016). Autophagy is a highly conserved biological process that enables cells to degrade and recycle damaged and misfolded proteins to maintain protein homeostasis (Amin, Perera, Beart, Turner, & Shabanpoor, 2020). Impairments in autophagy are thought to be critically important in the pathogenesis of ALS.

Mitochondrial dysfunction is another key feature of ALS. In ALS, motor neurons exhibit mitochondrial defects that result in decreased expression of ATP synthesis, increased production of reactive oxygen species (ROS), and disrupted calcium homeostasis (Giorgi et al., 2018; E. F. Smith, Shaw, & De Vos, 2019). These mitochondrial anomalies contribute to compromised energy production in affected neurons, oxidative stress, and excitotoxicity, all of which have been shown to impair motor neuron survival (Grosskreutz, Van Den Bosch, & Keller, 2010; E. F. Smith et al., 2019).

While the exact mechanism by which motor neurons degenerate in ALS remains to be fully understood, researchers have previously noted evidence that glutamate-mediated excitotoxicity plays a role in ALS. It has been postulated that elevated glutamate levels lead to excessive activation of glutamate receptors, causing an influx of calcium ions into neurons (Van Den Bosch, Van Damme, Bogaert, & Robberecht, 2006). Excessive calcium ion overload initiates a cascade of deleterious events, including mitochondrial dysfunction, oxidative stress,

and activation of cell death pathways, ultimately culminating in neuronal injury and death (Grosskreutz et al., 2010).

Neuromuscular junction (NMJ) integrity has been shown to be compromised early in the disease pathogenesis of ALS. NMJs are the synapses between motor neurons and muscle fibers, essential for the transmission of motor signals that induce muscle contraction. Research indicates that the presynaptic terminals of motor neurons degenerate, leading to reduced acetylcholine release and subsequent muscle denervation (Moloney, de Winter, & Verhaagen, 2014). This denervation is accompanied by a loss of postsynaptic acetylcholine receptors, further impairing neuromuscular transmission. The disruption of NMJs precedes the death of motor neurons and is thought to contribute to the progressive weakness and muscle atrophy characteristic of ALS (Campanari, Garcia-Ayllon, Ciura, Saez-Valero, & Kabashi, 2016; Kiernan et al., 2011). Additionally, the instability of NMJs has been linked to mutations in several ALS-related genes, which disrupt cytoskeletal dynamics and impair the maintenance of these critical synapses (Campanari et al., 2016).

Recent studies have highlighted the crucial role of neuroinflammation in the pathogenesis of ALS, suggesting that it is not merely a consequence but a driving factor in disease progression (Garofalo et al., 2022; J. Liu & Wang, 2017). One of the central components of neuroinflammation in ALS is the activation of microglia, the resident immune cells of the central nervous system (Muzio, Viotti, & Martino, 2021). Activated microglia release pro-inflammatory cytokines i.e., IL-1 $\beta$ , TNF- $\alpha$ , and IL-6, and ROS, which exacerbate neuronal damage (Clarke & Patani, 2020). This microglial activation is evident in both sporadic and familial cases of ALS and is associated with the presence of protein aggregates, such as TDP-43, in motor neurons (Bright, Chan, van Hummel, Ittner, & Ke, 2021). Furthermore, astrocytes, another type of glial

cell, play a significant role in the inflammatory response in ALS. Under pathological conditions, astrocytes can undergo a reactive transformation, contributing to the neurotoxic environment by releasing inflammatory mediators and failing to support neuronal health (Kwon & Koh, 2020; J. Liu & Wang, 2017). This dysfunction in astrocytes further amplifies neuroinflammatory signals and neuronal stress. Peripheral immune cells infiltrate the central nervous system in ALS, further intensifying inflammation (Z. Liu et al., 2020). Blocking these immune cells has shown promise in reducing neuroinflammation and slowing disease progression (Garofalo et al., 2022).

Recent advances in genetic screening and sequencing techniques, such as Genome-Wide Association Studies and Whole Exome Sequencing, have significantly expanded our understanding of ALS. Since 2016, these methodologies have identified 12 novel ALS-linked genes, providing new insights into the genetic underpinnings of the disease (Wang, Guan, & Deng, 2023). This ongoing research underscores the heterogeneity of ALS and highlights the potential for personalized therapeutic approaches tailored to specific carriers of genetic mutations. In summary, the pathophysiology of ALS encompasses a myriad of interrelated processes, including genetic mutations, protein aggregation, autophagic impairment, mitochondrial dysfunction, excitotoxicity, and neuroinflammation. Continued research into these mechanisms is crucial for the development of effective treatments and improving outcomes for individuals with ALS.

### 1.1.3 Clinical Manifestations of ALS

The clinical manifestations of ALS are heterogeneous within the patient populations (Orsini et al., 2015). Approximately 70% of ALS cases are classified as limb-onset, characterized by early symptoms such as focal limb weakness, spasticity, or muscle atrophy primarily affecting

the arms or legs. In contrast, about 30% of patients exhibit bulbar-onset ALS, marked by initial symptoms including dysarthria, dysphagia, and atrophy of the muscles coordinating the tongue (Kiernan et al., 2011; Masrori & Van Damme, 2020). A minority of patients may present with less common initial symptoms such as unintentional weight loss, respiratory insufficiency, or cognitive impairments indicative of frontal lobe dysfunction (Hardiman et al., 2017). Despite the initial site of onset, ALS invariably progresses to involve widespread motor neuron degeneration, leading to a relentless decline in neuromuscular function. Clinically, this progression is evident by increasing muscle weakness, spasticity, and atrophy, resulting in significant impairments in voluntary motor control (Kiernan et al., 2011; Oskarsson, Gendron, & Staff, 2018). As the disease advances, patients typically experience severe dysarthria, dysphagia, and ultimately, respiratory failure, which is the predominant cause of mortality within 2 to 5 years following diagnosis (Kiernan et al., 2011; Masrori & Van Damme, 2020).

The clinical diagnosis of ALS is often protracted, commonly requiring up to two years post-onset to properly diagnose due to other disorders of the nervous system being ruled out (Orsini et al., 2015). The absence of specific biomarkers and definitive tests makes the diagnostic process of ALS complex. Diagnosis is primarily clinical, guided by the El Escorial criteria (Brooks, 1994), which necessitate evidence of both upper and lower motor neuron degeneration, while also excluding other conditions that could mimic ALS, such as multiple sclerosis, neoplastic lesions, cerebrovascular accidents, spinal muscular atrophy, multifocal motor neuropathy, and neuromuscular junction disorders (Kiernan et al., 2011; Oskarsson et al., 2018). Understanding the full spectrum of ALS manifestations and diagnostic complexities is crucial for developing effective therapeutic strategies and improving patient outcomes. ALS encompasses diverse disease mechanisms involving both central and peripheral nervous system components,

with the prominence of these mechanisms varying according to specific genetic mutations, proteinopathies, and the progression of symptoms in patients (Goyal et al., 2020). Continued research into the molecular and cellular underpinnings of ALS is essential for identifying potential therapeutic targets, the creation of reliable biomarkers and developing interventions that can mitigate disease progression to enhance the quality of life for patients.

#### 1.1.4 Therapeutic Approaches for ALS Patients

The traditional treatment landscape for ALS is primarily centered around two main pharmacological interventions: riluzole and edaravone. Riluzole, the first FDA-approved drug for ALS, modulates glutamatergic neurotransmission by inhibiting presynaptic release and postsynaptic receptor activation, and is believed to prolong survival by three to six months (R. G. Miller, Mitchell, & Moore, 2012). More recently, edaravone, a free radical scavenger, has been approved as a therapy for ALS based on evidence demonstrating its ability to slow the decline in the ALS Functional Rating Scale (ALSFRS-R) score in patients (Neupane et al., 2023). Recently, Albriozza (AMX0035, Amylyx Pharmaceuticals), an agent formulated to alleviate endoplasmic reticulum and mitochondrial stress, has gained approval for administration in Canada. Studies have revealed its efficacy in decelerating the progression of the disease, as indicated by a 25% reduction in the decline of ALSFRS-R scores and an extension of lifespan by 6.5 months (Paganoni et al., 2022). Additionally, for individuals with mutations in SOD1, Tofersen, an antisense oligonucleotide (Biogen), has been authorized for therapeutic use. This marks a significant milestone as the first gene-specific medication approved for ALS treatment. Although Tofersen's efficacy is still being evaluated worldwide, initial findings suggest promise in mitigating the decline observed in ALSFRS-R scores (T. M. Miller et al., 2022).

Despite recent advancements, ALS treatment remains predominantly focused on symptom management. While the past few years have introduced two new drugs to the clinic, continued research into the underlying mechanisms of ALS is critical for the development of more effective and targeted therapies.

## **1.2 TANK-Binding Kinase 1 (TBK1)**

### 1.2.1 Structure of TBK1

Tumor necrosis factor (TNF) receptor associate factor NF $\kappa$ B (TANK)-binding kinase 1 (Tbk1), also known as NAK or T2K, is a serine/threonine kinase comprising 729 amino acids (Zhou, Zhang, & Xu, 2020). Structurally, TBK1 consists of four distinct domains, each with specialized functions (**Figure 1**). The serine/threonine kinase domain (KD) at its N-terminus is responsible for catalyzing phosphorylation events critical for signal transduction (Larabi et al., 2013). The KD contains an activation loop spanning from Leu164 to Gly199. The phosphorylation of Ser172 within this loop leads to the activation of TBK1 through autophosphorylation. Adjacent to the KD domain lies the ubiquitin-like domain (ULD), which plays a role in kinase activity of TBK1 and likely contributes to protein-protein interactions and substrate recognition (Larabi et al., 2013). The coiled-coil domain 1 (CCD1) harbors leucine zipper and helix-loop-helix domains that control the dimerization of the TBK1 molecule. The C-terminal coiled-coil domain 2 (CCD2) contains an adaptor-binding motif facilitating the interaction of TBK1 with its adaptors TANK, NAK-associated protein 1 (NAP1), Sintbad, optineurin (OPTN), and p62 (Larabi et al., 2013). These adaptor proteins regulate TBK1 by controlling its localization, activation, and participation in downstream signaling cascades (Fitzgerald et al., 2003; Goncalves et al., 2011).



**Figure 1** | Schematic of human TANK-binding kinase 1 (TBK1) primary structure. TBK1 spans 729 amino acids and is characterized by four main domains: a kinase domain (KD), a ubiquitin-like domain (ULD), and two coiled-coil domains (CCD1 and CCD2).

### 1.2.2 TBK1 in ALS

Two independent studies identified *TBK1* mutations in ALS patients through whole exome sequencing in European populations (Cirulli et al., 2015; Freischmidt et al., 2015). Subsequent research has further confirmed TBK1's involvement in ALS-FTD and identified *TBK1* mutations in patient cohorts worldwide. Mutations in *TBK1* are thought to account for about 1% of ALS cases but are implicated in up to 10% of cases where ALS co-occurs with frontotemporal dementia (ALS-FTD), indicating an overlap between these neurodegenerative disorders (Cirulli et al., 2015; Le Ber et al., 2015; Masrori & Van Damme, 2020). Moreover, *TBK1* mutations represent the fifth most commonly associated gene with ALS. Human genetic studies have identified nonsense, frameshift, missense, and deletion mutations in both sporadic and familial ALS cases dispersed throughout *TBK1* and do not cluster in specific domains (Cirulli et al., 2015; Freischmidt et al., 2015). These mutations are thought to confer a loss-of-function phenotype, leading to aberrant protein aggregation, impaired mitochondrial function, autophagic disruption, and neuroinflammation, all hallmark features of ALS pathology (Ahmad, Zhang, Casanova, & Sancho-Shimizu, 2016; Oakes et al., 2017). Nonsense and frameshift mutations disrupt expression of *TBK1*, implying that TBK1 haploinsufficiency may be the predominate mode of action in the development of TBK1-related ALS cases (Freischmidt et al., 2015).

### 1.2.3 Function of TBK1

TBK1 is a ubiquitously expressed serine/threonine kinase. As a constituent of the I-kappa-B kinase (IKK) family of proteins, TBK1 occupies a central regulatory role in innate immunity antiviral response, selective autophagy, mitophagy, and apoptosis (Zhou et al., 2020). TBK1 distinguishes itself from its fellow IKK family members in its unique role as a "noncanonical" I-kappa-B kinase, playing a more important role in inducing type-I and III interferon responses (Jin et al., 2012). Although its contribution to the production of Type I interferon (IFN) is prominent, TBK1 also mediates the generation of inflammatory cytokines via NF- $\kappa$ B activation. The activation of TBK1 involves a dynamic process where it undergoes trans-autophosphorylation within its homodimeric configuration subsequent to phosphorylation events initiated by upstream signaling cascades (Ma et al., 2012). Activation-induced conformational changes facilitate TBK1's interaction with adaptor proteins, notably TABK and NAP1, thereby culminating in the formation of multiprotein signaling complexes (Ma et al., 2012; Oakes et al., 2017). Consequently, TBK1 phosphorylates its downstream substrates, namely, interferon regulatory factors 3 (IRF3) and 7 (IRF7), promoting their nuclear translocation and subsequent expression of type I and III interferon (IFN) genes (Ahmad et al., 2016; Goncalves et al., 2011). These interferons, pivotal in immune orchestration during viral incursions, set forth a complex cascade of signal transduction. This includes not only the production of IFNs but also the expression of pro-inflammatory cytokines such as IL-1 $\beta$ , IL-6, and TNF- $\alpha$ , anti-inflammatory cytokines such as IL-10, and chemokines like IL-8, collectively regulating diverse immune interactions. Thus, they establish an antiviral milieu and coordinate the activities of innate and adaptive immune cells (Ahmad et al., 2016; Zhou et al., 2020)

TBK1 functions as the central kinase within the intricate network of signaling complexes mediated by TRIF, MAVS, and STING, orchestrating cellular responses to diverse stimuli (**Figure 2**) (S. Liu et al., 2015; Zhou et al., 2020). The TRIF pathway is initiated upon engagement of Toll-Like receptors (TLRs) by their respective ligands (Fitzgerald et al., 2003). Specifically, TLR3 recognizes double-stranded DNA (dsRNA) and TLR4 recognizes lipopolysaccharides (LPS) (Gatot et al., 2007; Jimenez-Dalmaroni, Gerswhin, & Adamopoulos, 2016). Upon ligand binding, the TRIF and TRAF3 adaptor proteins are recruited, facilitating the activation of TBK1 within a complex comprised of its associated proteins NAP1, SINTBAD, and TANK (Fitzgerald et al., 2003). Activated TBK1 subsequently phosphorylates IRF3 and IRF7, promoting their nuclear translocation and subsequent induction of type I and type III IFN genes, respectively (Ahmad et al., 2016). Furthermore, TBK1-mediated phosphorylation of TRIF amplifies the inflammatory response by facilitating the activation of NF- $\kappa$ B (H. Smith et al., 2011). Thus, the TRIF-TBK1 pathway bridges extracellular pathogen recognition and intracellular signaling cascades, culminating in the expression of antiviral and pro-inflammatory genes.

Conversely, the MAVS pathway triggers innate immune responses following the detection of viral RNA in the cytosol by RIG-1-like receptors (RLRs), specifically RIG-1 and MDA5 (Kawai et al., 2005). Upon recognition, MAVS forms prion-like aggregates, recruiting TBK1 to the mitochondrial membrane for activation (Hou et al., 2011; Seth, Sun, Ea, & Chen, 2005). TBK1-mediated phosphorylation of MAVS enhances its stability and signaling activity, thereby augmenting antiviral responses (Seth et al., 2005). Activation of TBK1 at the mitochondria subsequently leads to the phosphorylation of IRF3, IRF7, and NF- $\kappa$ B, facilitating

the expression of interferons and pro-inflammatory cytokines to coordinate immune defense against RNA viruses (Hou et al., 2011; Seth et al., 2005).

The STING pathway is activated in response to cytosolic DNA, a hallmark of viral infections and cellular stress (Chen, Sun, & Chen, 2016). DNA is sensed by cyclic GMP-AMP synthase (cGAS), resulting increase in cGMP levels (Wu et al., 2013). The activated STING recruits TBK1 to the endoplasmic reticulum (ER) to activate TBK1 (Zhao et al., 2019). Furthermore, TBK1-mediated phosphorylation of STING itself enhances its ability to activate downstream signaling molecules, potentiating antiviral responses (Zhao et al., 2019). This STING-TBK1 pathway is critical for protection against DNA viruses and aberrant self-DNA.

Through phosphorylation of key downstream effectors, TBK1 orchestrates the expression of antiviral genes and inflammatory mediators to shape the immune response to diverse pathogens and environmental cues such as oxidative stress, ER stress, and mitochondrial dysfunction. While it remains to be fully understood how environmental insults impact the pathogenesis of ALS, TBK1 mutations may compromise cellular responses to inflammatory stress, contributing to neuronal degeneration and disease progression. Further research is necessary to elucidate the precise mechanisms by which TBK1 dysfunction intersects with environmental factors to influence ALS onset and progression.

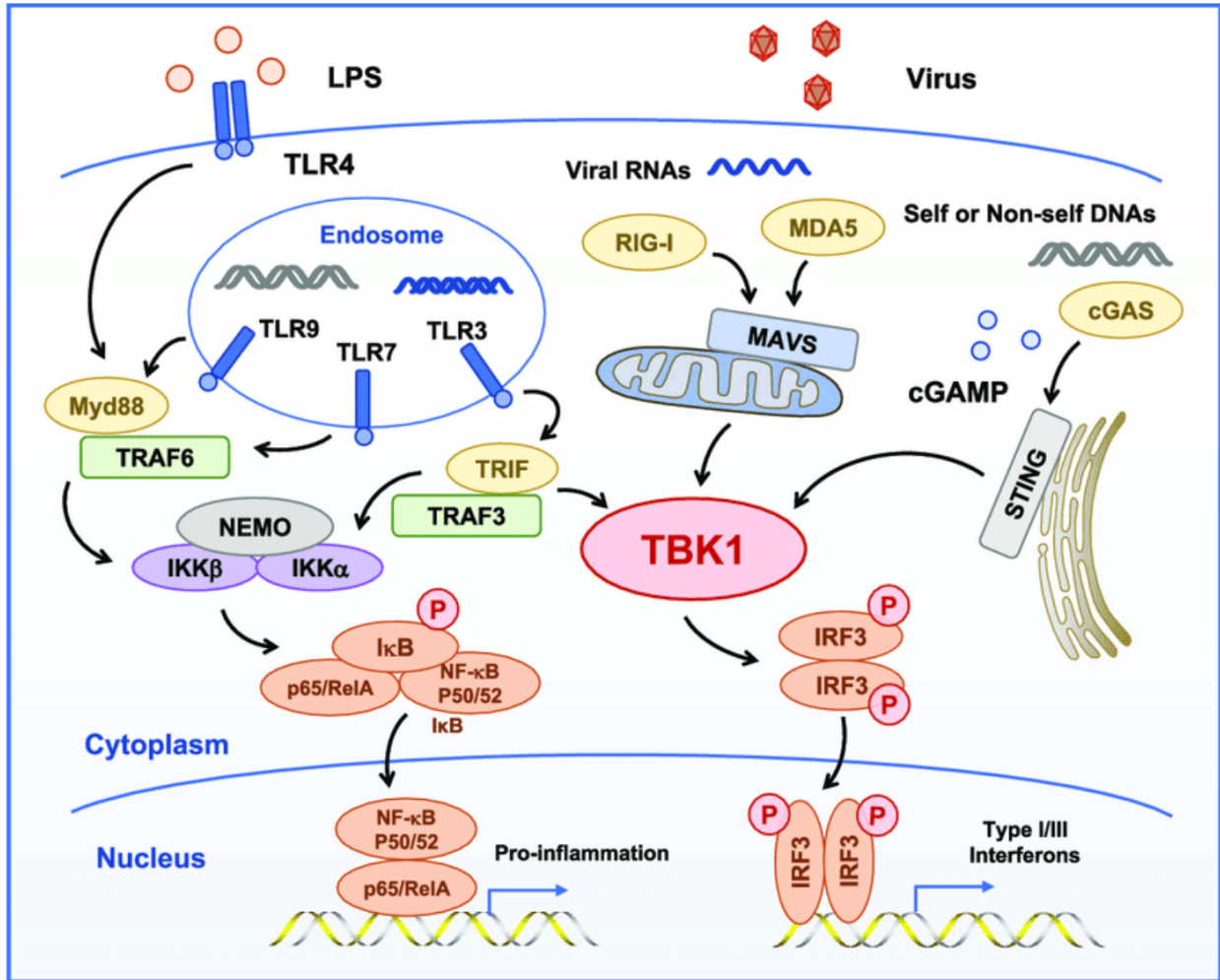


**Figure 2** | Schematic representation of TBK1 involvement in inflammation induction. Figure taken from: (Zhou et al., 2020)

In addition to its functions in innate immunity, TBK1 directly influences autophagy, acting as both a positive and negative regulator depending on the nature of the stimuli or pathological conditions present (Herhaus, 2021; Weidberg & Elazar, 2011). Recent evidence underscores the mechanism through which proteins involved with autophagy recognize and bind specific cargo (Gatica, Lahiri, & Klionsky, 2018). This process entails concurrent binding to ubiquitin residues on target cargo *via* their ubiquitin-binding domain, as well as to phosphatidylethanolamine-conjugated microtubule-associated protein light chain 3 (LC3-II)

proteins embedded in the autophagosomal membrane (Gatica et al., 2018; Oakes et al., 2017). In post-mitotic cells, notably neuronal cells, autophagy assumes an indispensable role as a survival mechanism for the elimination of protein aggregation, given the inability of these cells to dilute aberrant proteins through cell division (Valencia, Kim, Jang, & Lee, 2021). TBK1-mediated phosphorylation of selective autophagy receptors such as optineurin (OPTN), p62, nuclear dot protein 52 kDa (NDP52), and neighbour of BRCA1 gene 1 (NBR1), enhances their affinity for ubiquitinated cargo and facilitates their recruitment to autophagosomes for degradation (Oakes et al., 2017).

TBK1 emerges as a pivotal regulator of mitophagy, the process dedicated to the clearance of damaged mitochondria. Upon loss of the mitochondrial membrane potential, PINK1 stabilizes on the outer mitochondrial membrane (OMM) and phosphorylates ubiquitin, attracting Parkin to tag mitochondria for degradation (Heo, Ordureau, Paulo, Rinehart, & Harper, 2015). TBK1 then phosphorylates OPTN at the OMM, enhancing its binding to ubiquitin chains. OPTN then recruits the autophagy adaptors, including the ULK1 complex, to form a double-membraned phagophore that engulfs the damaged mitochondrion (Heo et al., 2015; Lazarou et al., 2015). This process involves the incorporation of LC3 into the phagophore, with TBK1-mediated phosphorylation of OPTN facilitating its interaction with LC3-II. The engulfed mitochondrion undergoes degradation following the fusion of the phagophore with lysosomes (Lazarou et al., 2015).

TBK1's involvement in programmed cell death arises from its regulatory influence on Receptor-interacting protein kinase 1 (RIPK1), a central mediator in balancing cell survival and death (D. Xu et al., 2018). Deubiquitinated RIPK1 can interact with RIPK3 to form the necrosome, promoting necroptosis, or recruit FADD and caspase-8 to facilitate apoptosis (Lafont

et al., 2018). Phosphorylation of RIPK1 by TBK1 inhibits its function, thereby modulating cell death. Consequently, dysregulation of TBK1 can precipitate aberrant programmed cell death. Interestingly, research by D. Xu et al. (2018) revealed that the expression of TAK1, a kinase regulator of RIPK1, decreases in the aging human brain. This decrease may heighten the aged brain's sensitivity to TBK1 dysregulation, which inhibits RIPK1 activity. This sensitivity could potentially link to the adult onset of ALS. Furthermore, TBK1 indirectly modulates RIPK1 by dictating inflammatory responses and autophagy, thereby influencing RIPK1's proclivity to promote either apoptosis or necroptosis (Lafont et al., 2018; D. Xu et al., 2018).

### **1.3 Animal Models of TBK1**

#### **1.3.1 Mouse Models of TBK1**

Murine models are the most widely studied *in vivo* models of ALS, as human TBK1 protein shares 99% homology with its mouse ortholog (Tojima et al., 2000). However, characterization of TBK1 function *in vivo* remains a challenge, as homozygous deletion of *Tbk1* in mice results in embryonic lethality at E14.5 due to severe hepatic tissue loss and apoptosis (Bonnard et al., 2000). Homozygous mice with a truncated *Tbk1* gene lacking kinase activity can survive (Marchlik et al., 2010), as well as mice containing a conditional deletion of *Tbk1* in neurons. The conditional neuronal *Tbk1* deletion in mice has been shown to induce several neuropathological changes including reduced dendritic spine density, cortical spinal loss, and abnormal dendritic projections (W. Duan et al., 2019). However, loss of *Tbk1* specifically in motor neurons is not associated with a neurodegenerative disease phenotype (Gerbino et al., 2020).

Notably, mice with only one copy of the *Tbk1* (hemizygotes) do not display any symptoms unless they also carry the ALS-linked SOD1<sup>G93A</sup> variant (Brenner et al., 2019). In these mice, they experience early-stage autophagy problems and faster muscle denervation. However, in later stages, there is a reduction in microglial neuroinflammation, leading to a slower disease progression and longer survival. Conversely, conditional knockout of *Tbk1* in motor neurons of SOD1<sup>G93A</sup> mice increases the aggregation of SOD1 and accelerates the onset of the disease without impacting lifespan (Brenner et al., 2019; Gerbino et al., 2020). Furthermore, a study using a mouse model with a hemizygous deletion of *Tbk1* and expressing the human TDP-43<sup>G298S</sup> ALS variant revealed that the absence of one *Tbk1* gene exacerbated muscle denervation without impacting motor neuron loss or spinal cord gliosis (Sieverding et al., 2021). This underscores the importance of TBK1 in maintaining motor neuron health.

### 1.3.2 Zebrafish Model of TBK1

Zebrafish (*Danio rerio*), are an excellent vertebrate model to study disease as their organization of tissues and organs, including the brain and spinal cord, are largely conserved with mammals. Furthermore, its genome contains orthologs for over 80% of human disease-causing genes (Babin et al., 2014; Howe et al., 2013). They regularly produce hundreds of externally fertilized embryos that are relatively easy to genetically manipulate (Babin et al., 2014; Howe et al., 2013). Sexual maturity is reached at 3 months of age, and they are optically transparent during larval stages of development, making them easy to image (Howe et al., 2013). Zebrafish *Tbk1* shares 71% identity and 81% similarity with its human ortholog (**Figure 3**). As a vertebrate, zebrafish possess cytokines involved in neuroinflammation, including IL-1 $\beta$ , IL-6,

and TNF- $\alpha$ , making zebrafish a good model for studying neuroinflammatory processes relevant to the study of human diseases, including ALS (Babin et al., 2014).

TBK1_human	mqstsnhlwllsdilgqgatanvfrgrhkktgdlfaikvfnnisflrpvdvqmrefevlk	60
Tbk1_zebrafish	mqstanylwmmssdlgqgatanvyrggrhkktgdyavkvfnnlsflrpldvqmrefevlk ****:*	60
TBK1_human	klnhknivklfaieeetttrhkvlimefcpcgslytvleepsnayglpeseflivlrdvv	120
Tbk1_zebrafish	klnhknivklfaveeesnrhkvlmeycpcgslytvleeptnayglpedeflivlqdvv *****:*	120
TBK1_human	ggmnhlrengivhrdikpgnimrvigedgqsvykltdfgaareleddeqfvslygteeyl	180
Tbk1_zebrafish	agmnhlreygivhrdikpgnimrvigddgfsvykltdfgaareleddeqfvslygteeyl ***** *****:*:* *****	180
TBK1_human	hpdmyeravlrkdhqkkygatvdlwsigvtfyhaatgslpfrpfegprnrkevmykiitg	240
Tbk1_zebrafish	hpdmyeravlrkdhqkkygatvdlwsigvtfyhaatgslpfrpfegprnrkevmykiite *****	240
TBK1_human	kpsgaisgvqkaengpidwsgdmpvscslsrqlvlltpvlanileadqekcwgdqffa	300
Tbk1_zebrafish	kppgaisghqkfengkiewssempiscslskglqsltpvlanileadqekcwgdqffa ** ***** ** ** *:*:*:*:*:* *****	300
TBK1_human	etsdilhrmvi hvfslqqmtahkiyhsyntatifhelvykqtkiissngeliyegrrlv	360
Tbk1_zebrafish	etsdilhrivvyvfslqqatlhvvyihtyntanlfqellfrtrnitpshqellyegrrlv *****:*:*:****** *:*:*:*:*:*:*:*:*:*:*:* *:*:*:*:******	360
TBK1_human	lepgrlaqhfpkttteenpifvvsreplntigliyekislpkvhprydlgdasmakaitg	420
Tbk1_zebrafish	ldpnrqagtfpktsrdnpimllcrdpvntvgllfedpsppkvqprydlldasyaktfag *:*.* ** *****:*:*:*:*:*:*:*:*:*:*.* * ***** ** ** *:*:*	420
TBK1_human	vvcyacriastllyqelmrkgirwlielikddynetvhkktevvitldfcirniektvk	480
Tbk1_zebrafish	dvgylwktsdslllyqelvrkgvrglnelirdeysetmhkktevfhlchscsqtlrseq * * : ::*:*:*:*:*:*:* * *****:*:*:*:******. . * * : : * : *	480
TBK1_human	vyeklmkinleaaelgeisdihtklrlrslssqgtietslqdidrslspggs ladawahqe	540
Tbk1_zebrafish	lcealmqgnilsaeydeirdtrkklrslsgslasmdqtlqdinsmflpggsltdwtqgv : * ** : * : ** .** * :*:*:******. : : : * : * : * : * : * : *	540
TBK1_human	gthpkdrnveklqvllncmteiyqfkkdkaerrlayneeqihkfdkqklyyhatkamth	600
Tbk1_zebrafish	gthpedrnvekikvlldaigaiyqfkkdkaerrlpynneeqihkfdkqkvlvhatkaral *****:*****:*:*:*:* * ***** ***** ***** *	600
TBK1_human	ftdecvkkyaeflnkseewirkmlhrlrkqllsltnqcfdieevskyqeytnelqetlpq	660
Tbk1_zebrafish	ftdecamkyrlfiskseewmkkfhvrkhllsltgqfssleqevtllmqrylkllleqfpq *****. *. *:*:*:*:*:*:* *:*:*:******. :*:*:*: : * * : **	660
TBK1_human	kmftassgikhtmtpiypsntlvemtlgmkkk keemegvvkelaennhilerfgsltmd	720
Tbk1_zebrafish	kvvpmasgvlpk--qaylspstlvemtlgmkkk keemegvvkelaennflerfgsltvd *:. :*:*: : * * .***** ***** :*****:*	718
TBK1_human	gglrnvdcl 729	
Tbk1_zebrafish	gmrtrverm 727 **:*:*: :	

**Figure 3** | Amino acid sequence comparison between human TBK1 and zebrafish Tbk1. Zebrafish Tbk1 shares 71% identity and 81% similarity with human TBK1 amino acid sequence.

## **2. Materials and Methods**

### **Zebrafish Husbandry**

Adult Tübingen long fin (TL) zebrafish (*Danio rerio*) were bred, raised, and maintained in accordance with standard protocols (Westerfield, 1995) at 28.5°C in a 14/10-hour light/dark cycle in the animal research facility of the Montreal Neurological Institute (MNI), associated with McGill University (Montreal, Quebec, Canada). All experiments were performed in compliance with the guidelines of the Canadian Council for Animal Care and approved by the MNI's Animal Care Committee.

### **Cas9 mRNA and Guide RNA Synthesis**

To replicate a mutation analogous to one identified in an ALS patient from the Montreal Neurological Institute, several guide RNAs (gRNAs) targeting the coding region of exon 11 were designed. The human missense mutation, *TBK1*<sup>A417X</sup>, corresponds to the zebrafish mutation *tbk1*<sup>A419X</sup>. CRISPRscan was utilized to identify multiple gRNA target sites in the *tbk1* locus. The selected gRNA targets were synthesized with the T7 MEGAscript kit (Invitrogen) and purified via phenol-chloroform extraction followed by ethanol precipitation. A zebrafish codon-optimized Cas9 (pT3TS-nCas9n, Addgene plasmid # 46757) was linearized using XbaI overnight, and 1 µg of the linear template DNA served as the basis for in vitro mRNA transcription using the T3 mMESSAGE mMACHINE® (Invitrogen) kit. The resulting mRNA was purified by phenol-chloroform extraction and ethanol precipitation for purification. The gRNA target site for *tbk1*, located on the 3' to 5' reverse strand in exon 11, is as follows, with the protospacer-adjacent motif (PAM) underlined: GGACACCTTTTGTAGTCTAAGAG

## **CRISPR/Cas9 Mutagenesis and Screening for Founder Lines**

Heterozygous *tbk1* knockouts (KOs) were generated following the procedures established in previous research (Armstrong et al., 2016). The synthesized gRNA (100 ng/μL) was co-injected with *Cas9* mRNA (100 ng/μL) into one-to-two-cell stage zebrafish embryos at ~2 nL volumes. Assessment of DNA cutting efficiency was evaluated through high-resolution melting (HRM) analysis on 24 one-to-two-day-post-fertilization (1-2 dpf) embryos per gRNA target. The gRNA demonstrating the highest efficiency was selected to establish a zebrafish line with disrupted *tbk1* reading frames. F0 adults were crossed with wild-type (WT) zebrafish, and the resulting embryos were screened for indel transmission via HRM.

HRM primer sequences for verification of *tbk1* line:

Forward: 5' TTCGCAGGTGATGTGGGATACCT 3'

Reverse: 5' TGTACCAATCCAGTTAGGGTTGAT 3'

## **General genotype screening and knockout generation**

Adult zebrafish were isolated and anesthetized using 1% tricaine (MS-222, Sigma). DNA was extracted from a caudal fin clip using the Extract-N-Amp™ Tissue PCR Kit (Millipore Sigma), and target sites were amplified via polymerase chain reaction (PCR) followed by HRM analysis. Sequencing of the amplicons (Genome Québec) confirmed the specific mutation of each founder line: a single nucleotide deletion in exon 11 (6918G > del), resulting in a frameshift mutation and the creation of a premature stop codon (W425X) in the open reading frame. Founder zebrafish carrying this frameshift mutation resulting in premature stop codons in the *tbk1* gene were selected, and F1s were incrossed to generate the *tbk1* homozygous KOs.

Sanger Sequencing Primer Sequences for verification of *tbk1* line:

Forward: 5' TTCGCAGGTGATGTGGGATACCT 3'

Reverse: 5' CGGATCTCGTCATACTCGGC 3'

### ***In vitro* fertilization of zebrafish eggs**

The *in vitro* fertilization methodology was adapted and refined based on the protocol outlined by Draper and Moens (2009). Adult zebrafish, aged between 6 months to 1 year, were gently anesthetized using a 0.04% solution of MS-222 (Sigma-Aldrich) dissolved in system water. To prevent premature hydration and swelling of the extracted eggs, female fish were carefully blotted dry before being positioned upside down on a folded plastic sheet (4 x 6 cm). Eggs were then extruded by applying gentle pressure with the thumb just above the cloaca area. High-quality eggs, identifiable by their yellow color and dry texture, were selectively collected using a spatula and transferred to a 35 mm petri dish. In cases where a sufficient number of eggs were required for successful fertilization, multiple females were pooled together. Similarly, to avoid premature activation of sperm cells, male zebrafish were also blotted dry and positioned upside down in a foam holder. Sperm extraction was performed under a microscope by gently squeezing the area anterior to the cloaca towards the cloaca itself, utilizing fine-tipped, untextured forceps (Fisher Scientific). High-quality sperm, characterized by its white color and non-watery consistency, was collected using an aspirator fitted with a gel loading tip (0.6 mm O.D., Fisher Scientific), which was calibrated at every  $\mu\text{L}$ . To ensure an adequate volume of sperm for fertilization, samples from several males were pooled together until a minimum of 1  $\mu\text{L}$  was obtained.

Fertilization of the eggs was achieved by introducing the collected sperm and activating it with 300  $\mu$ L of system water, followed by a 5-minute incubation period at room temperature (23°C). Subsequently, 4 mL of system water was added, and the fertilized eggs were then allowed to incubate for 3 hours at 28°C. Upon completion of the incubation period, the fertilized eggs were carefully transferred to 40 mL culture bottles and maintained at 28°C until they were ready for use in experiments or until they reached maturity.

### **Survival analysis of zebrafish larvae**

Heterozygous *tbk1* KO zebrafish were incrossed and the offspring were monitored over a 15 dpf period. During this 15-day period, the genotypic frequencies of the offspring were assessed at intervals of 2, 5, 10, and 15 dpf. The DNA of individual larvae was extracted, and genotyping was performed using PCR followed by HRM analysis. To determine if the observed genotypic frequencies deviated from the expected Mendelian ratios (1:2:1 for WT (*tbk1*<sup>+/+</sup>), *tbk1*<sup>+/-</sup>, and *tbk1*<sup>-/-</sup>, respectively), a chi-squared ( $\chi^2$ ) test was employed. This statistical test compared the observed counts of each genotype to the expected counts under the hypothesis of Mendelian inheritance. Any significant deviation from the expected Mendelian ratios would suggest an impact of the *tbk1* knockout on viability.

### **2 dpf larval motor function**

Larval motor function was assessed using a touch response analysis previously described by our lab. Individual larvae aged 52-54 hours post-fertilization (hpf) were placed at the center of a 150 mm Petri dish filled with fresh system water, with the water temperature maintained between 24 °C and 25 °C. After allowing a habituation period of 30-60 seconds, the larvae's tail

was gently touched with forceps to trigger a burst swimming response. The larval movement was recorded from an overhead perspective at a frame rate of 30 Hz (Grasshopper 2 camera, Point Gray Research). Recording continued until the larvae either ceased movement or reached the dish perimeter. Total swim time, total swim distance, mean swim velocity, and maximum swim velocity were quantified using the frame-by-frame manual tracking software (Manual Tracking plugin, ImageJ).

### **8 dpf larval motor function**

Individual larvae aged 8 dpf were placed into individual wells of a specialized 24-well plate filled with system water maintained at a temperature of 28.5 °C. The well plate was then placed inside the DanioVision (Noldus) apparatus for monitoring and analysis of larval behaviour. Following a 30-minute habituation period, larval motion was recorded for a duration of one hour. The recorded data was analyzed for mean swim velocity of individual larvae using EthoVision CT software (Noldus).

### **Neuromuscular Junction Colocalization**

Immunofluorescence microscopy, a protocol involving double labeling of pre-synaptic and post-synaptic membranes, was utilized to evaluate the integrity of neuromuscular junctions (NMJs). Synaptotagmin 2 (Syt2) antibodies were employed to mark pre-synaptic sites, while sulforhodamine-conjugated alpha-bungarotoxin (a-Btx) targeted post-synaptic membranes, following previously described methods (Armstrong & Drapeau, 2013). First, 10 dechorionated zebrafish larvae at 2 dpf were fixed in 4% paraformaldehyde (PFA) prepared in phosphate-buffered saline (PBS) overnight at 4 °C with gentle rotation. The fixed larvae were then washed

three times with PBS, each for 15 minutes, followed by a 45-minute incubation at room temperature (RT) in 1 mg/mL collagenase solution in PBS. After another round of PBS washes (3 x 15 minutes), the larvae were treated with PBST (PBS with Triton X-100) for 30 minutes at RT and subsequently incubated in 10 mg/mL sulforhodamine-conjugated a-Btx in PBST for 30 minutes at RT.

Subsequent steps included rinsing the larvae with PBST (3 x 15 minutes) and incubating them in a fresh blocking solution (composed of 2% goat serum, 1% bovine serum albumin (BSA), 0.1% Triton X-100, and 1% DMSO in PBS) for an hour at RT. The larvae were then left overnight in the blocking solution containing the primary Syt2 antibody (DSHB, diluted 1:100). The following day, the larvae were washed with PBST (4 x 15 minutes) and incubated for 5 hours at RT in a fresh blocking solution containing the Alexa Fluor 647 secondary antibody (ThermoFisher, diluted 1:1200). The larvae underwent final washes with PBST (3 x 15 minutes), then incubated in PBST overnight at 4 °C with gentle rotation. Lastly, the larvae were transferred to a 70% glycerol solution and mounted on glass slides for imaging. The NMJs were then visualized using a Quorum Technologies microscope equipped with a 60x/ 1.42 oil immersion objective and an 89 NORTH LDI spinning disk confocal mounted on an Olympus BX61W1 fluorescence microscope. A Photometrics Prime BSI camera captured the images, which were processed using Volocity software (Improvision).

### **Adult Free Swim Assay**

1.5-year-old adult zebrafish were placed into a white, square open field test arena (29.3 cm x 29.3 cm) with system water maintained between 27-29 °C throughout all trials. Following a 5-minute acclimatization period, the zebrafish were recorded from a top-down perspective for 5

minutes (Flir camera). The recorded videos were analyzed with EthoVision software (Noldus) to evaluate the mean swim velocity of each fish. Additionally, EthoVision software was used to generate heatmaps for each fish, illustrating their total movement during the trial.

### **Adult Swim Tunnel Assay**

1.5-year-old adult zebrafish were placed into a swim tunnel system (Loligo Systems) with system water maintained between 27-29 °C and subjected to a sprint test ( $U_{max}$ ) to assess their anaerobic swimming capacity. During the test, the water velocity was incrementally increased by 5 cm/s every minute. Following the point of failure, when the zebrafish could no longer maintain their position against the flow, they were promptly removed from the swim tunnel and weighed. The  $U_{max}$  value was determined using the equation  $U_{max} = U_f + U_s \times (t_f / t_s)$ , where  $U_f$  represents the water velocity of the last fully completed interval,  $U_s$  is the increment of water velocity per interval,  $t_f$  is the time spent in the final interval before the fish could no longer swim against the current, and  $t_s$  is the duration of each interval.

### **Larval RNA Extraction**

At 2 dpf, 8-10 dechorionated larvae were placed in a single tube and homogenized for 2 minutes at 4 °C. The RNA was then extracted using ARCTURUS PicoPure RNA Isolation Kit (Applied Biosystems), following the specified protocol. To eliminate residual DNA, the extracted RNA was treated with DNase I (Qiagen) in accordance with the guidelines provided by the manufacturer. Subsequently, the quality and concentration of the RNA was assessed using a NanoDrop Lite® spectrophotometer.

### **Adult Tissue RNA Extraction**

Brain samples from adult zebrafish were homogenized for 30 seconds at 4 °C. The RNA was then extracted using ARCTURUS PicoPure RNA Isolation Kit (Applied Biosystems), following the specified protocol. To eliminate residual DNA, the extracted RNA was treated with DNase I (Qiagen) in accordance with the guidelines provided by the manufacturer. Subsequently, the quality and concentration of the RNA was assessed using a NanoDrop Lite® spectrophotometer.

### **Quantitative Reverse Transcription PCR (RT-qPCR)**

2.5 µg of RNA was used to create a cDNA library using the SuperScript VIOLA cDNA Synthesis Kit (Invitrogen). Quantitative real-time PCR (RT-qPCR) was performed on each cDNA library using the SYBR Green Supermix (Bio-Rad Laboratories), with expression levels of each sample measured in triplicates. The delta-delta Ct method of relative quantification for each gene analyzed was normalized to *gapdh* in larval qPCR experiments and *ef1a* for adult qPCR experiments.

Primer Sequences for RT-qPCR analysis of *tbk1*:

Forward: 5' AAGCTGTTCGCCGTCGAG 3'

Reverse: 5' CATCACCAGCACCTTATGACG 3'

Primer Sequences for RT-qPCR analysis of *irf3*:

Forward: 5' GCAGATTGAATGGAGATCCGTCT 3'

Reverse: 5' CAGGTACAGCTCCTAAATGTGGT 3'

Primer Sequences for RT-qPCR analysis of *irf7*:

Forward: 5' TTCAGGGTCAACATTATCGCAGC 3'

Reverse: 5' TTGCTTTGTCGTTAGGATACTCG 3'

Primer Sequences for RT-qPCR analysis of *p62*:

Forward: 5' CGATGTTTTTGTTCGGTCTCA 3'

Reverse: 5' CAAGAGCCAAACCCATCATT 3'

Primer Sequences for RT-qPCR analysis of *optn*:

Forward: 5' GAATGGGGACATTAGTCACCCA 3'

Reverse: 5' TTCTCATCAGTTTCTGCTCGG 3'

Primer Sequences for RT-qPCR analysis of *ndp52*:

Forward: 5' TTCAGACCTGTAAAGAAGCCTGC 3'

Reverse: 5' GTCTGTAGATGTGTATTCAGTGGAGG 3'

Primer Sequences for RT-qPCR analysis of *nbr1*:

Forward: 5' CAAGAACGCAAAAGACAAGTCTCAC 3'

Reverse: 5' CTTGAAAATGGCTCAAGCCGAA 3'

Primer Sequences for RT-qPCR analysis of *ripk1*:

Forward: 5' GCAGATCTGATCAAGAAAGAGCCTC 3'

Reverse: 5' TCCAAGATTTCCAGAATGATCCTCC 3'

Primer Sequences for RT-qPCR analysis of *ifn $\phi$ 1*:

Forward: 5' AAAGCTCTGCGTCTACTTGC 3'

Reverse: 5' AGGTCAGACGATTTTCTGTGCA 3'

Primer Sequences for RT-qPCR analysis of *il-1 $\beta$* :

Forward: 5' GGCAATATGAAGTCACCATAGCTCCA 3'

Reverse: 5' CACCAGAGACTTCTTATACTGATCGC 3'

Primer Sequences for RT-qPCR analysis of *il-6*:

Forward: 5' TGCTATTCCTGTCTGCTACACTG 3'

Reverse: 5' TCTGAAGGTTTGAGGAGAGGAGT 3'

Primer Sequences for RT-qPCR analysis of *il-8*:

Forward: 5' GCTGGATCACACTGCAGAAA 3'

Reverse: 5' TGCTGCAAACCTTTTCCTTGA 3'

Primer Sequences for RT-qPCR analysis of *il-10*:

Forward: 5' AGTCCAACGATGACTTGGAACC 3'

Reverse: 5' AAGCTCCCCCATAGCTTTATAGACC 3'

Primer Sequences for RT-qPCR analysis of *tnf $\alpha$* :

Forward: 5' GGAAAGCTGGATCTTCAAAGTCG 3'

Reverse: 5' GCCATCATCGGGAATGATAATCTCC 3'

Primer Sequences for RT-qPCR analysis of *nfkb1*:

Forward: 5' AAACCTCGCGTTGATCTCGA 3'

Reverse: 5' GACTTGCGGTTCTTCTCGCT 3'

### **Sublethal LPS Response RT-qPCR Assay**

2 dpf zebrafish larvae were bathed in a sublethal concentration (50 µg/ mL) of *Pseudomonas aeruginosa* LPS dissolved in system water as previously described (Novoa et al., 2009). Following a 2-hour bath exposure to LPS, larvae will be collected for RNA extraction and RT-qPCR analysis using the primers listed above.

### **Statistical Tests**

All statistical analyses were performed using Prism 9 (GraphPad Software Inc.). The normality of sample distributions was assessed using the Shapiro-Wilks test. For comparisons involving two samples, unpaired Student's t-tests were employed. Kruskal-Wallis tests were used to compare data sets containing more than two non-normally distributed samples, followed by Dunn's post-hoc multiple comparisons test. One-way ANOVA, followed by Tukey's multiple comparisons test, was applied to normally distributed datasets with more than two samples. Chi-squared tests were used to compare genotypic frequencies. Significance was determined at a threshold of  $p < 0.05$ .

### **3. Results**

#### **Generation CRISPR KO line of zebrafish *tbk1*: *tbk1*<sup>+/-</sup> and *tbk1*<sup>-/-</sup> zebrafish lines**

A zebrafish *tbk1* KO line was generated using CRISPR/Cas9-mediated genome editing. The zebrafish *tbk1* gene is composed of 20 exons (**Figure 4A**). To replicate a mutation analogous to one identified in an ALS patient from the Montreal Neurological Institute, several guide RNAs (gRNAs) targeting the coding region of exon 11 were designed and assessed. The human missense mutation, *TBK1*<sup>A417X</sup>, corresponds to the zebrafish mutation *tbk1*<sup>A419X</sup>. High-resolution melt (HRM) analysis of the F1 generation identified the most efficient gRNA, which facilitated the highest rate of DNA cleavage. Sanger sequencing subsequently revealed a single nucleotide deletion in exon 11 (6918G > del), resulting in a frameshift mutation and the creation of a premature stop codon (W425X) within the open reading frame. This indel mutation was confirmed via HRM analysis and was successfully transmitted to subsequent generations. Homozygous *tbk1* knockout zebrafish (*tbk1*<sup>-/-</sup>) were produced by in-crossing the F1 offspring.

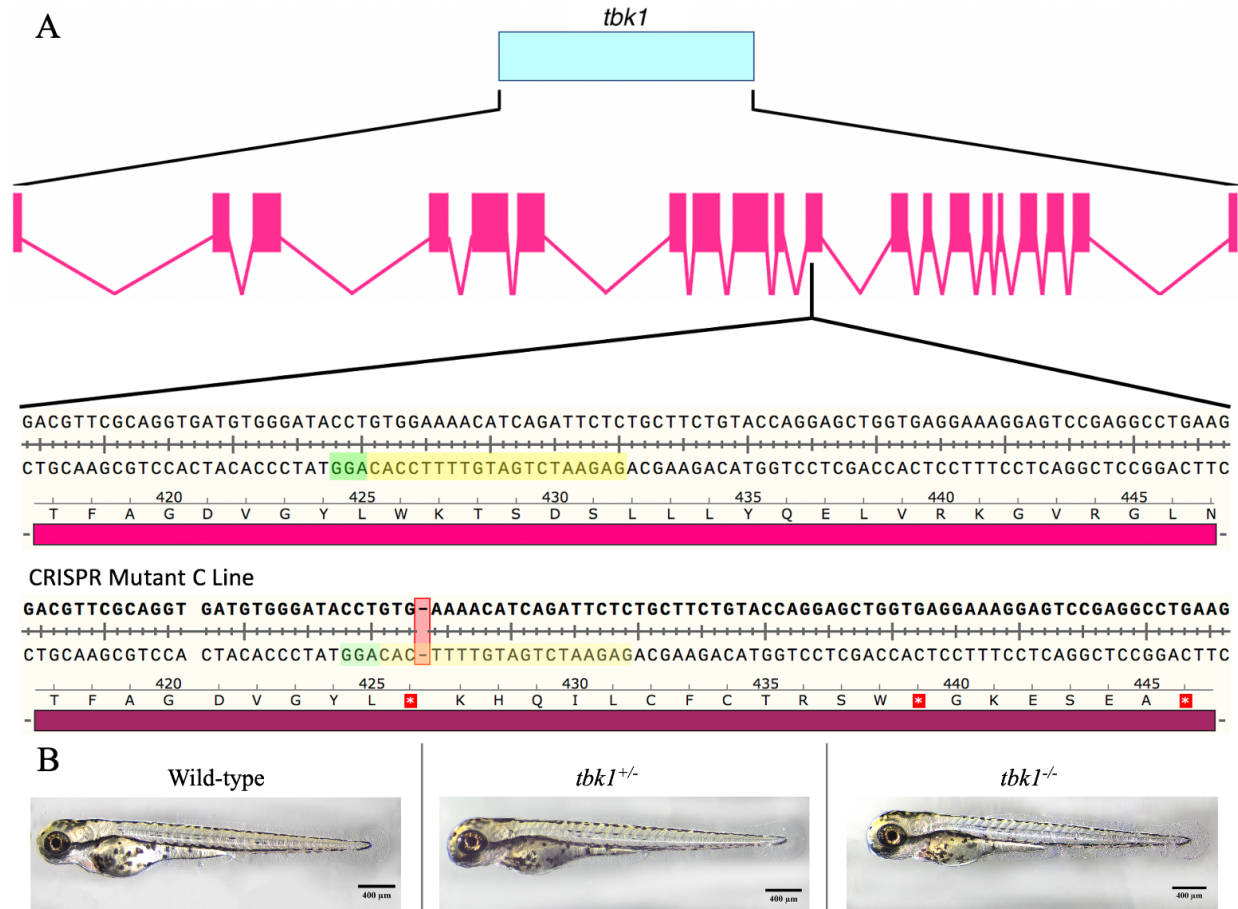


**Figure 4A** | Schematic representation of the genetic structure of zebrafish *tbk1* indicating location and type of indel introduced by CRISPR/cas9 mutagenesis to compare the WT reference sequence. **4B** | Example images of WT, heterozygous (*tbk1*<sup>+/-</sup>), and homozygous (*tbk1*<sup>-/-</sup>) zebrafish larvae at 3 dpf.

### Heterozygous *tbk1* KO line results in nonsense-mediated decay

The nonsense mutation introduces multiple premature stop codons within the transcript, prompting the hypothesis that it may significantly disrupt *tbk1* transcript expression levels. To investigate this, we conducted an RT-qPCR analysis to quantify *tbk1* expression in cDNA synthesized by using RNA collected from whole brains. More specifically, we measured *tbk1* expression levels in the brains of adult WT (*tbk1*<sup>+/+</sup>) and heterozygous (*tbk1*<sup>+/-</sup>) zebrafish, using *efl1a* as the normalization control. Additionally, we assessed *tbk1* expression in 5 dpf larvae, with

normalization against *gapdh* expression, to ensure accurate and reliable comparisons across developmental stages.

I observed that both adult brains and whole larval *tbk1*<sup>+/-</sup> zebrafish expressed approximately half the amount of *tbk1* compared to their WT counterparts. This substantial reduction in *tbk1* expression suggests that the CRISPR/Cas9-induced nonsense mutation induces nonsense-mediated decay (NMD) of the *tbk1* transcript. The significant decrease in *tbk1* transcript levels observed in both developmental stages underscores the impact of the mutation on gene expression and the effectiveness of the NMD pathway in mitigating aberrant mRNA translation (Figure 5).

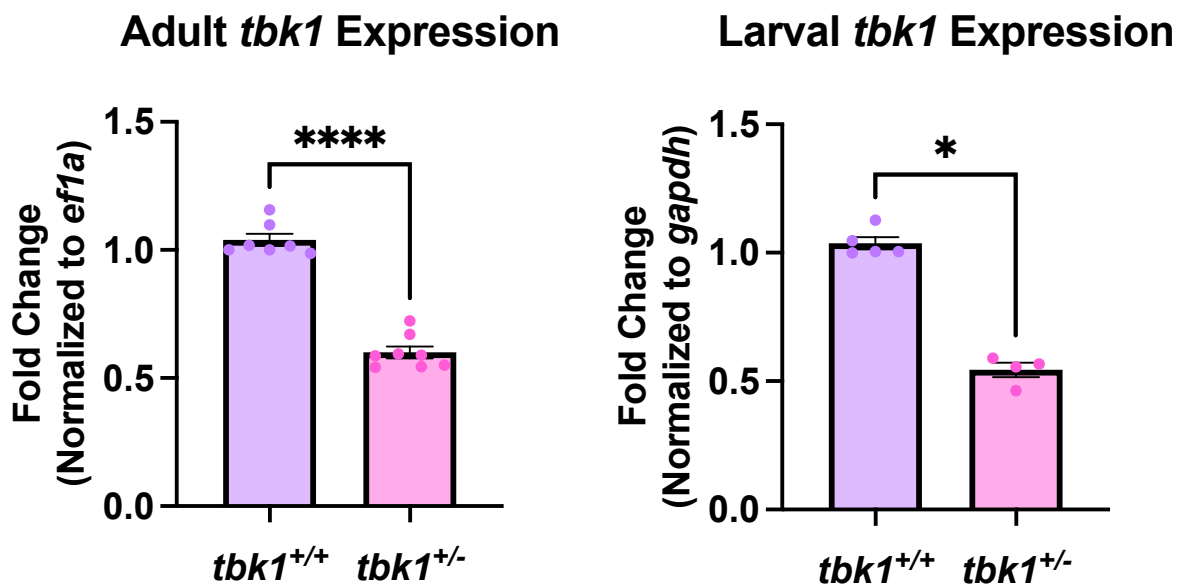


**Figure 5** | RT-qPCR analysis of *tbk1* expression in 1.5-year-old adults and 5 dpf larvae demonstrates reduced levels of *tbk1* transcript in heterozygous knockouts. n = 7 for WT, n = 8 for adult *tbk1*<sup>+/-</sup> brains., n = 5 for WT, n = 4 for *tbk1*<sup>+/-</sup> 5 dpf larvae. For adult *tbk1* expression,  $t(13) = 13.26$ ,  $p < 0.0001$ . For larval *tbk1* expression, Mann-Whitney  $U = 0$ ,  $p = 0.02$ . (\*\*\*\*) indicates  $p < 0.0001$  and (\*) indicates  $p < 0.05$ .

## **Homozygous *tbk1* KOs display reduced survival despite no morphological differences at larval stages of development**

Previous investigations into the role of Tbk1 in the context of ALS have predominantly relied on cell or murine KO models of Tbk1. Notably, homozygous *Tbk1* knockout mice exhibit embryonic lethality by embryonic day 14.5 (E14.5), thereby complicating the analysis of TBK1's functional consequences and indicating a critical developmental role for this gene (Bonnard et al., 2000). Zebrafish (*Danio rerio*), with their externally fertilized embryos, offer a unique model to circumvent these limitations.

I hypothesized that the *tbk1*<sup>-/-</sup> zebrafish would also display reduced viability. In accordance with Mendelian genetics principles, the expected outcome of a heterozygous *tbk1*<sup>+/-</sup> incross would yield a progeny ratio of 25% WT, 50% *tbk1*<sup>+/-</sup>, and 25% *tbk1*<sup>-/-</sup> zebrafish. However, upon genotyping the larvae that reached sexual maturity, *tbk1*<sup>-/-</sup> zebrafish, which should have been present in the expected Mendelian ratio, were conspicuously absent.

This unexpected absence prompted a comprehensive investigation into the viability of *tbk1*<sup>-/-</sup> zebrafish larvae. Our analysis showed that the *tbk1*<sup>-/-</sup> zebrafish exhibit a severely compromised lifespan, failing to survive beyond 15 dpf (**Figure 6**). This outcome underscores the essential role of TBK1 during early development and provides a crucial insight into its functional significance.

## Survival Percentages by Genotype

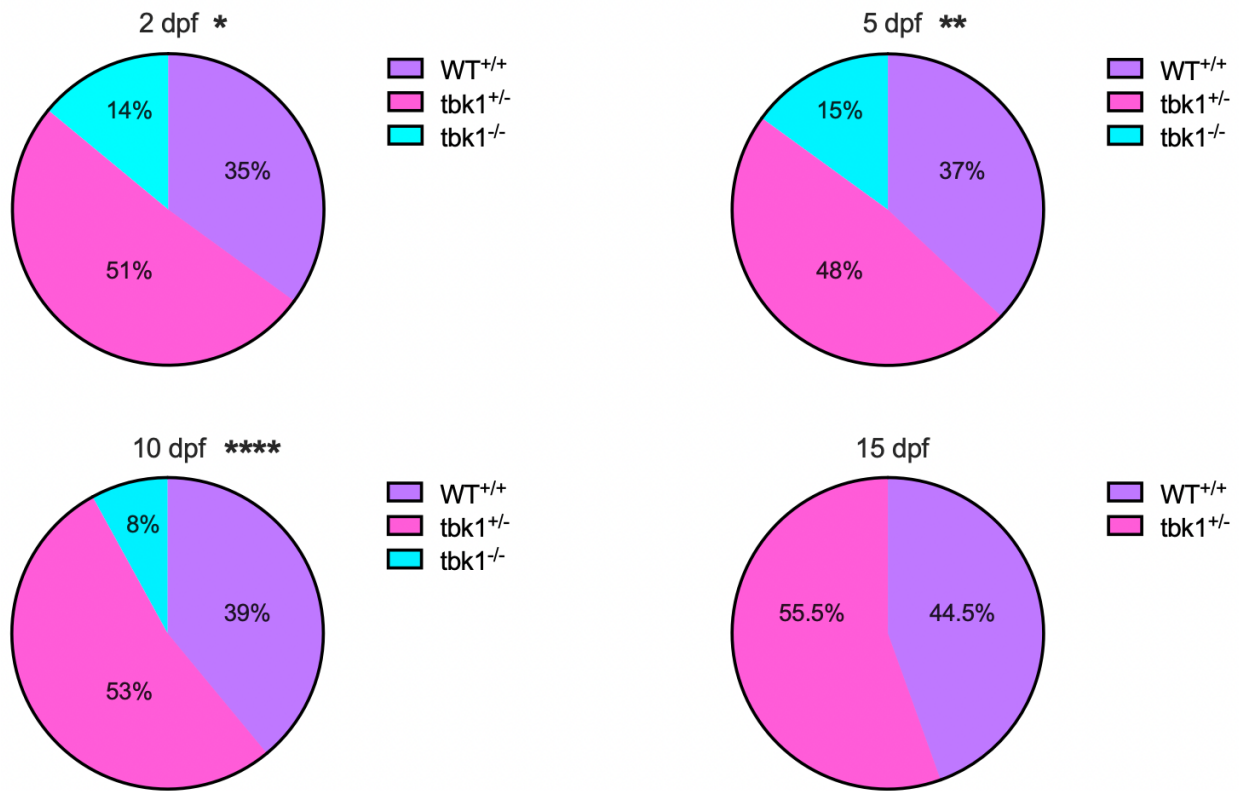


**Figure 6** | Genotypic frequency of WT, *tbk1*<sup>+/-</sup>, and *tbk1*<sup>-/-</sup> zebrafish larvae at 2, 5, 10, and 15 dpf following a parental heterozygous *tbk1*<sup>+/-</sup> incross. Homozygous *tbk1* knockout larvae display early lethality and are not observed to survive past 15 dpf. At 2 dpf,  $\chi^2 = 8.86$ ,  $p = 0.01$ . At 5 dpf,  $\chi^2 = 9.84$ ,  $p = 0.007$ . At 10 dpf,  $\chi^2 = 19.58$ ,  $p < 0.0001$ .

### Homozygous *tbk1* KO larvae exhibit a hyperactive motor function phenotype at 2 dpf

Given the debilitating nature of ALS, characterized by progressive motor dysfunction, this study aimed to investigate motor function anomalies within our *tbk1* model. Zebrafish larvae at 2 dpf predominantly exhibit burst swimming escape responses when stimulated tactilely, making this developmental stage particularly suitable for evaluating early locomotor functions (Burgess & Granato, 2007).

Therefore, this study focused on assessing the larval touch responses of *tbk1* KO zebrafish, hypothesizing that these may reveal subtle yet significant alterations in motor behaviour, potentially preceding the more prominent phenotypic traits that emerge in later developmental stages and adulthood. Utilizing a touch response assay, the research aimed to discern whether heterozygous and/or homozygous *tbk1* KO impacted burst swimming patterns of larval zebrafish.

The analysis assessed several parameters of motor function: swim duration, swim distance, mean swim velocity, and maximum velocity in WT, *tbk1*<sup>+/-</sup>, and *tbk1*<sup>-/-</sup> larvae (**Figure 7**). Strikingly, homozygous *tbk1* knockout larvae exhibited a significant increase in swim duration at 2 dpf compared to their WT siblings. This prolonged swim duration in *tbk1*<sup>-/-</sup> larvae underscores the presence of aberrant motor function at this critical developmental stage. Notably, trends toward increased swim distance and decreased mean and maximum swim velocities in *tbk1*<sup>-/-</sup> larvae at 2 dpf were observed, further validating the manifestation of motor deficits. Importantly, no significant differences in motor function were detected between WT and *tbk1*<sup>+/-</sup> larvae at 2 dpf, highlighting the specificity of motor phenotypes in homozygous *tbk1* knockout zebrafish at this early developmental stage.

## 2 dpf Larvae Touch Response Analysis to *tbk1* Genotypes

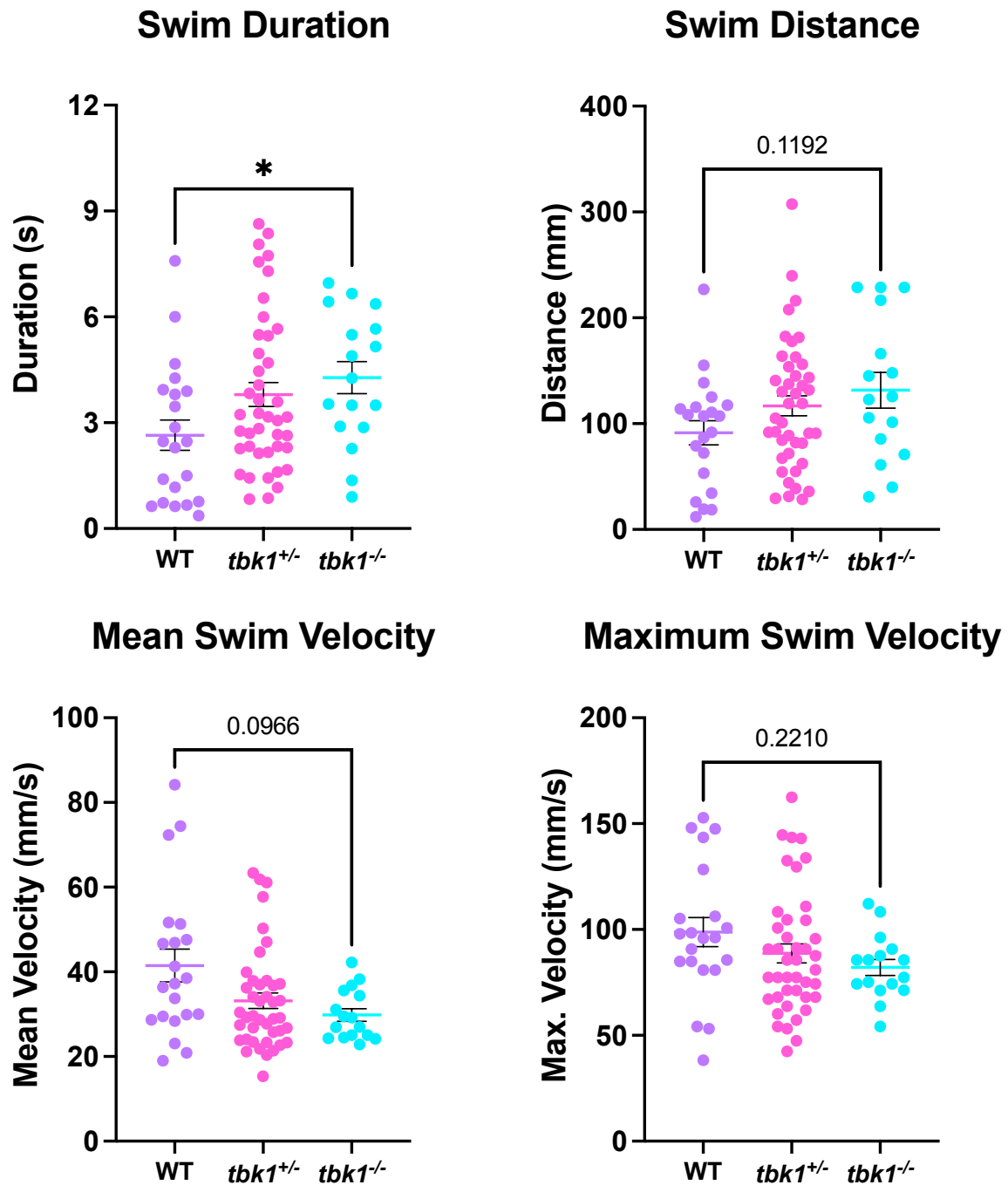


**Figure 7** | Excitable motor activity in *tbk1* KO larvae at early stages of motor development. Total swim duration, total swim distance, mean swim velocity, and maximum swim velocity for 2 dpf WT, *tbk1*<sup>+/-</sup>, and *tbk1*<sup>-/-</sup> zebrafish larvae. n = 21 for WT, n = 42 for *tbk1*<sup>+/-</sup>, and n = 17 for *tbk1*<sup>-/-</sup>.

The data set was analyzed with a one-way ANOVA followed by Tukey's multiple comparison tests. (\*) indicates  $p < 0.05$ . Non-significant p-values are indicated in graph comparisons above.

### Homozygous *tbk1* KO larvae exhibit a significant reduction in motor function at 8 dpf

By 8 dpf, zebrafish larvae have undergone significant maturation of their motor systems, characterized by the development of a distinctive beat-and-glide swimming pattern (Roussel, Gaudreau, Kacer, Sengupta, & Bui, 2021). This pattern of motor activity persists throughout the lifespan of the fish. Utilizing the DanioVision system, I assessed wild-type, *tbk1*<sup>+/-</sup>, and *tbk1*<sup>-/-</sup> zebrafish larvae at this critical developmental stage. The results indicated that the *tbk1*<sup>-/-</sup> larvae exhibited a markedly reduced mean swim velocity in comparison to both WT and *tbk1*<sup>+/-</sup> larvae. These findings highlight the crucial role of the *tbk1* gene in regulating motor function and suggest that its absence severely impairs the swimming capabilities of zebrafish larvae.

### Mean Swim Velocity of 8 dpf Larvae

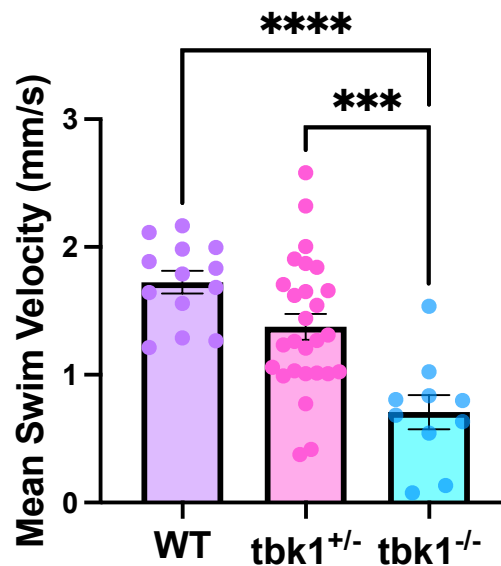


**Figure 8** | Mean swim velocity for 8 dpf WT, *tbk1*<sup>+/-</sup>, and *tbk1*<sup>-/-</sup> zebrafish larvae. n = 13 for WT, n = 27 for *tbk1*<sup>+/-</sup>, and n = 10 for *tbk1*<sup>-/-</sup>.  $F(2,29) = 5.2$ ,  $p = 0.01$ . When comparing *tbk1*<sup>-/-</sup> to WT,  $p = 0.03$  and  $p = 0.03$  when comparing *tbk1*<sup>-/-</sup> to *tbk1*<sup>+/-</sup> KOs. The data set was analyzed with a

one-way ANOVA followed by Tukey's multiple comparisons tests. (\*\*\*) indicates  $p < 0.001$  and (\*\*\*\*) indicates  $p < 0.0001$ .

### ***tbk1*<sup>+/-</sup> larvae present decreased colocalization of pre- and post-synaptic markers**

To further elucidate the underlying mechanisms contributing to the aberrant motor function observed in the *tbk1*<sup>-/-</sup> larvae at 2 and 8 dpf, NMJ structural integrity was assessed. Previous studies on ALS-mutant zebrafish models have reported compromised NMJ integrity, characterized by receptors being described as 'orphaned' when either pre-synaptic or post-synaptic puncta in the ventral root branching area lacked colocalization (Armstrong & Drapeau, 2013; Bose, Armstrong, & Drapeau, 2019). Utilizing sulforhodamine-conjugated  $\alpha$ -bungarotoxin, a postsynaptic marker binding to nicotinic acetylcholine receptors (nAChRs), in conjunction with an antibody targeting synaptic vesicle glycoprotein2A (SV2), a presynaptic marker, I evaluated NMJ morphology in WT, *tbk1*<sup>+/-</sup>, and *tbk1*<sup>-/-</sup> larvae following fixation in 4% PFA at 2 dpf (**Figure 9**).

The analysis focused on the presence of presynaptic and postsynaptic orphan puncta, which serve as indicators of disrupted synaptic connectivity. ImageJ software was utilized for this quantification. Remarkably, the *tbk1*<sup>-/-</sup> larvae exhibited a substantial increase in both presynaptic and postsynaptic orphan puncta when compared to the WT and *tbk1*<sup>+/-</sup> larvae (**Figure 9**). This significant rise in orphaned puncta underscores the pronounced disruption in NMJ integrity associated with the *tbk1*<sup>-/-</sup> genotype, thereby providing insights into the physiological basis of the observed motor function abnormalities.

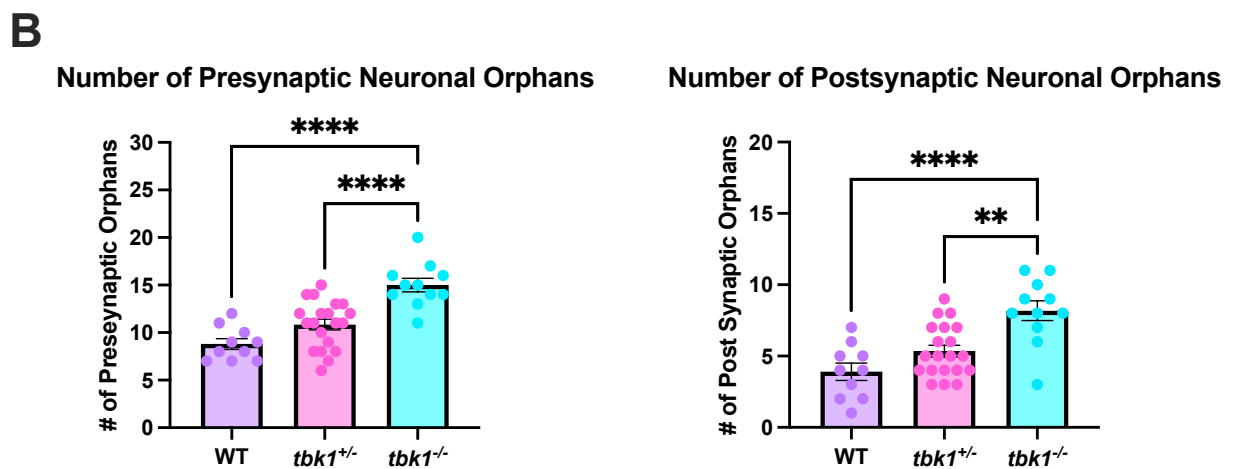
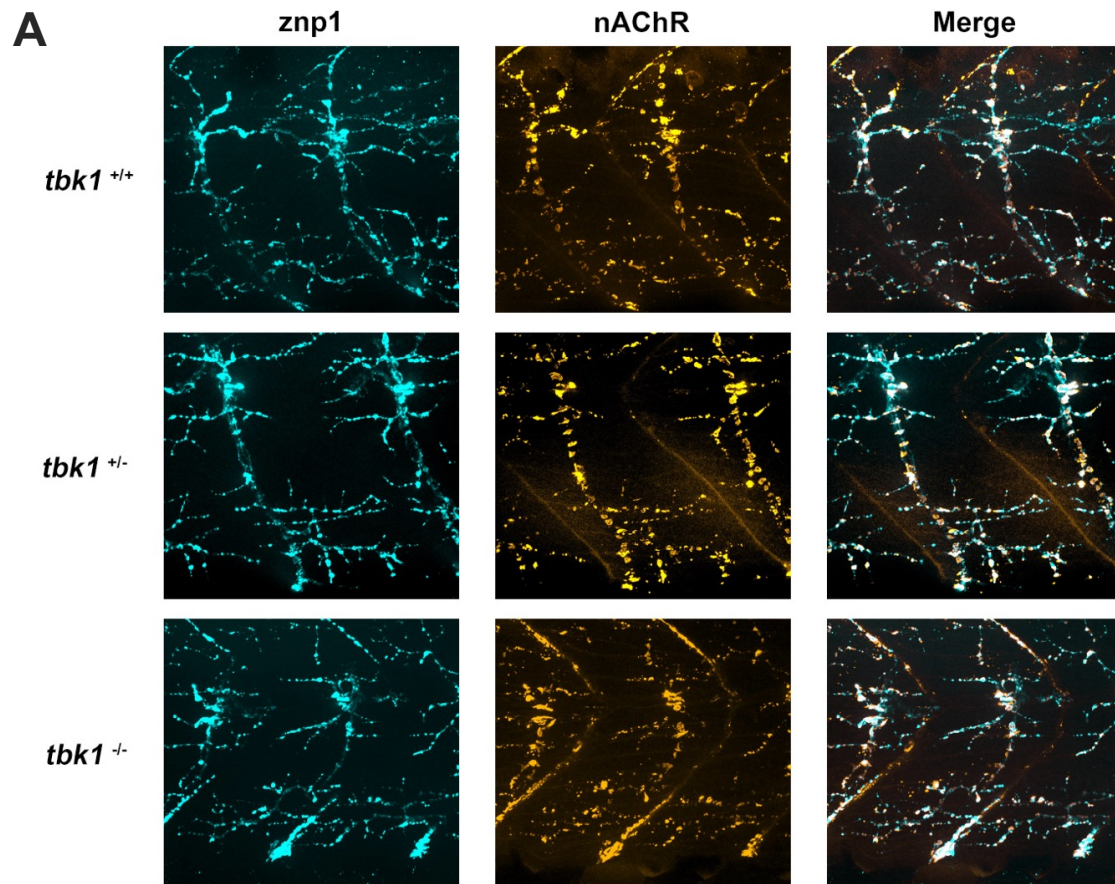


**Figure 9A** | Representative images depicting the branching of trunk ventral root projections for neuromuscular junction colocalization analysis in 2 dpf larvae. The top row shows WT larvae, the second row shows *tbk1*<sup>+/-</sup> larvae, and the third row shows *tbk1*<sup>-/-</sup> larvae. Cyan (left column) indicates syt2-labeled pre-synaptic terminals, gold (middle column) represents  $\alpha$ -bTx-labeled post-synaptic terminals, and the merged images are displayed in the right column. **9B** |

Quantification of orphaned pre-synaptic and post-synaptic terminals. The analysis demonstrates that homozygous *tbk1* knockout larvae exhibit a significantly higher number of orphaned pre-synaptic terminals and post-synaptic receptors compared to both WT and *tbk1*<sup>+/-</sup> larvae. Sample sizes were n = 10 for WT, n = 20 for *tbk1*<sup>+/-</sup>, and n = 11 for *tbk1*<sup>-/-</sup>. For orphaned presynaptic puncta,  $F(2,38) = 20.51$ ,  $p < 0.0001$ , and significant differences between homozygous KOs and both *tbk1*<sup>+/-</sup> and WT larvae were observed ( $p < 0.0001$ ). For orphaned postsynaptic puncta,  $F(2,38) = 13.06$ ,  $p < 0.0001$ , with  $p < 0.0001$  when comparing *tbk1*<sup>-/-</sup> to WT larvae and  $p = 0.001$  when comparing *tbk1*<sup>-/-</sup> to *tbk1*<sup>+/-</sup> larvae. Statistical analyses were performed using a one-way ANOVA followed by Tukey's multiple comparisons test. Statistical significance is denoted as (\*\*) for  $p < 0.01$  and (\*\*\*\*) for  $p < 0.0001$ .

### **Heterozygous *tbk1* adult zebrafish do not display a motor phenotype at 1.5 years old**

Given that ALS typically manifests as a late adult-onset disease, our investigation was extended to evaluate locomotor function in adult zebrafish at 1.5 years of age, encompassing both WT and *tbk1*<sup>+/-</sup> zebrafish. To achieve a comprehensive assessment, we utilized swim tunnel and free-swim assays, which allowed us to measure the maximum swimming speed ( $U_{\max}$ ) and the mean swim velocity (cm/s) across the different genotypes, respectively (**Figure 10**). The swim tunnel assay provided a controlled environment to evaluate the endurance and maximum sustained swimming capabilities, while the free-swim assay offered insights into natural, spontaneous swimming behaviors. Remarkably, the analysis revealed no significant differences in locomotor performance between the WT and *tbk1*<sup>+/-</sup> zebrafish at this advanced age. Both groups demonstrated comparable  $U_{\max}$  values and mean swim velocities, indicating that the hemizygous loss of *tbk1* did not impair motor function under the conditions tested. This suggests that the deletion of a single *tbk1* allele is insufficient to induce a discernible motor phenotype in adult zebrafish, which might be due to compensatory mechanisms or the need for additional genetic or environmental factors to manifest the motor deficits typically associated with ALS.

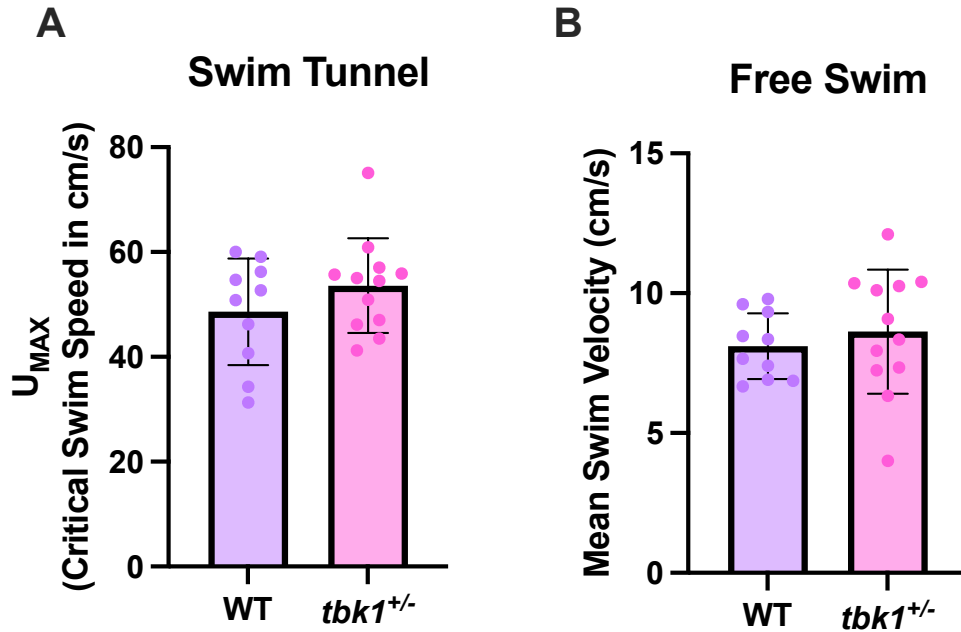


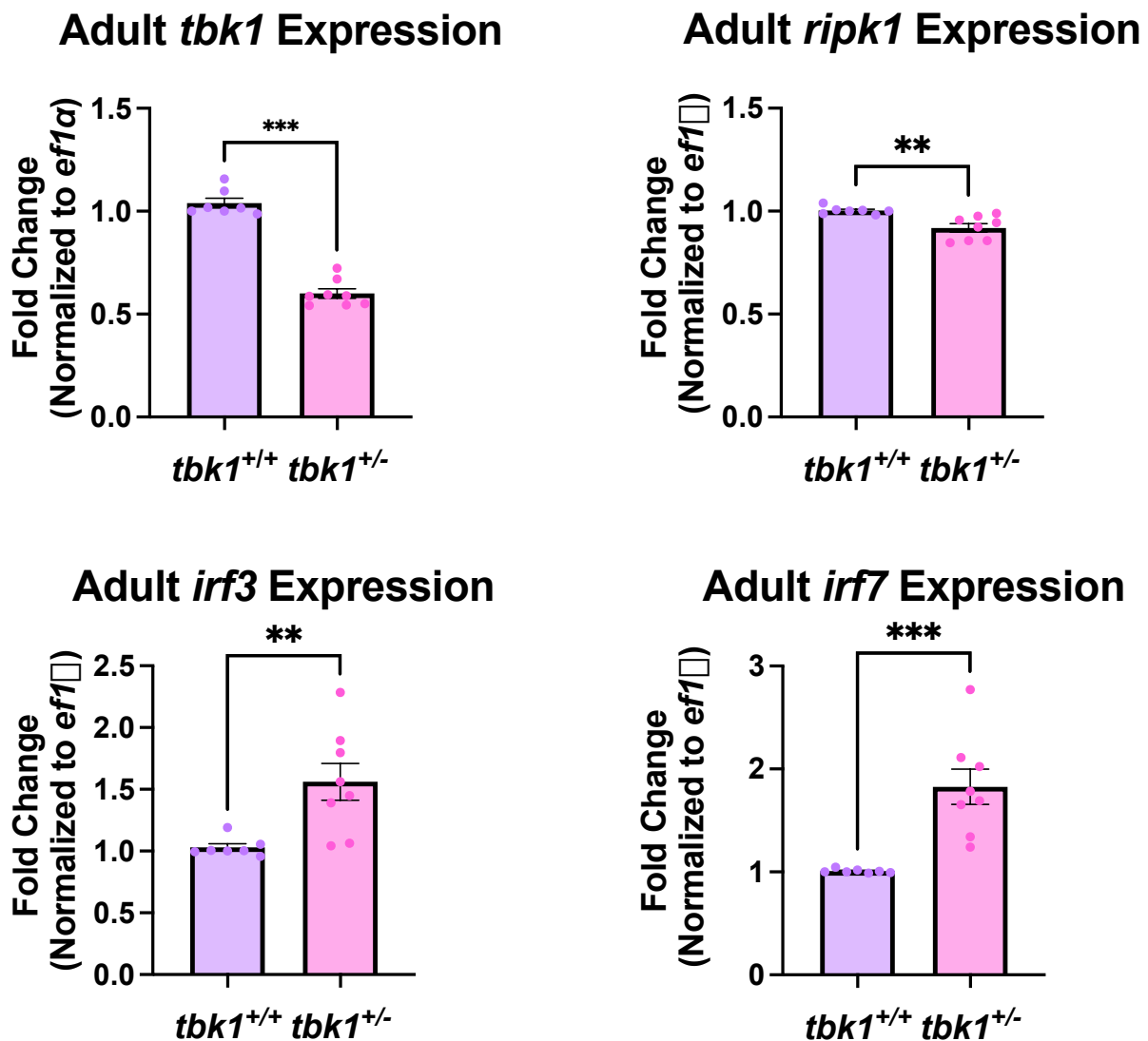
**Figure 10A** | Locomotor activity of 1.5-year-old WT and *tbk1*<sup>+/-</sup> zebrafish. A) Maximum sustained swimming capabilities of 1.5-year-old zebrafish adults.  $U_{max}$  (cm/s) was calculated using a swim tunnel (Loligo Systems).  $t(20) = 1.22$ ,  $p = 0.24$ .  $n = 10$  for WT and  $n = 12$  for *tbk1*<sup>+/-</sup> adults. **10B** | Mean velocity of 1.5-year-old adults.  $t(20) = 0.67$ ,  $p = 0.51$ .  $n = 10$  for WT and  $n = 12$  for *tbk1*<sup>+/-</sup> adults.

### Heterozygous *tbk1* adult zebrafish display aberrant immune responses at 1.5 years old

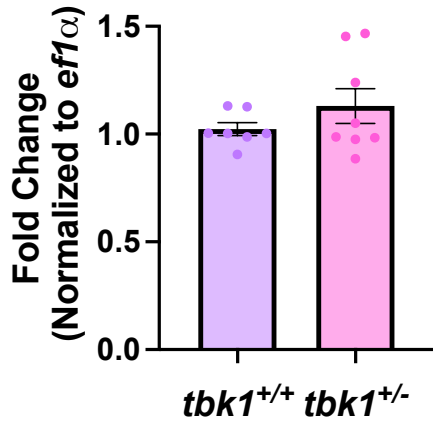
The involvement of TBK1 in the neuroinflammatory signaling pathway marks a significant milestone in understanding ALS. To delve into the transcriptional ramifications of heterozygous *TBK1* knockout, a model resembling the genetic makeup found in an ALS patient with a *TBK1*-associated ALS mutation, an in-depth analysis of inflammatory and autophagic gene expression profiles within the TBK1 signaling pathway was conducted.

Through RT-qPCR analysis, the expression levels of transcripts expression levels implicated in neuroinflammation and autophagy regulation were quantified. Among the target genes investigated were *p62*, *optn*, *ndp52*, *nbr1*, *ripk1*, *il1 $\beta$* , *il6*, *il10*, *irf3*, *irf7*, *ifn $\phi$ 1*, *nf $\kappa$ b1*, and

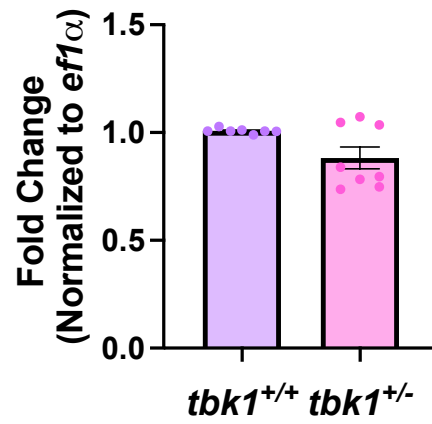
*tnfa*. The comparative analysis revealed distinct alterations in gene expression patterns between WT and *tbk1*<sup>+/-</sup> zebrafish. Notably, a significant downregulation was observed in the expression of *ripk1*, *optn*, *il8*, and *il10* in the heterozygous zebrafish when compared to their wild-type counterparts (**Figure 11**). Conversely, there was a significant upregulation in the expression of *p62*, *irf3*, and *irf7* in the heterozygous *tbk1* zebrafish. These findings underscore the complex regulatory interplay between *tbk1* and downstream effectors involved in the modulation of immune responses, autophagy, and apoptosis.



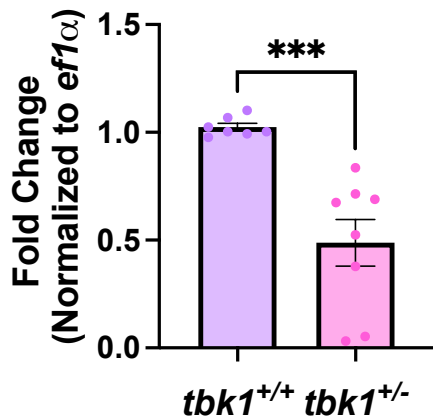
**Adult *il1 $\beta$*  Expression**



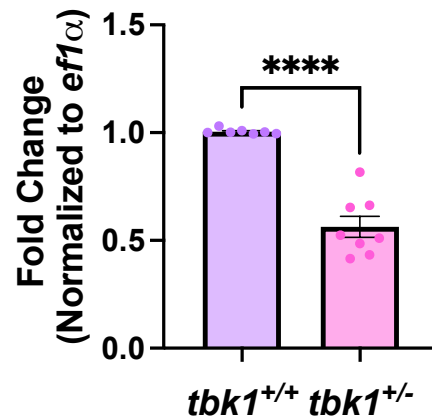
**Adult *il6* Expression**



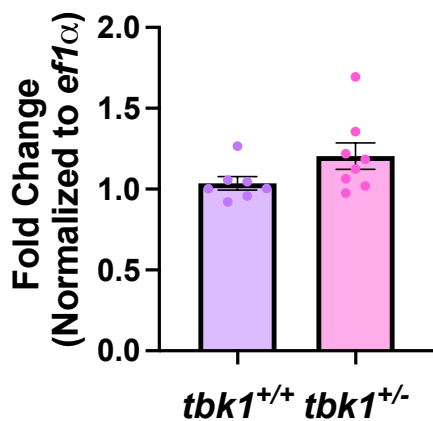
**Adult *il8* Expression**



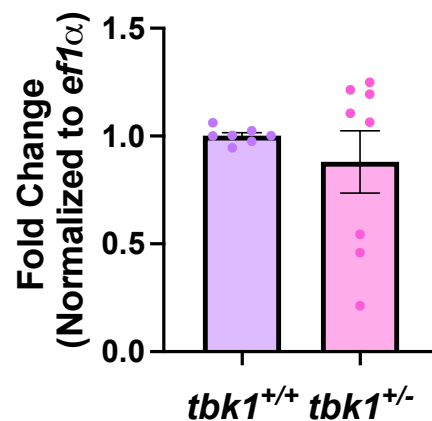
**Adult *il10* Expression**



**Adult *tnf $\alpha$*  Expression**



**Adult *nfκb1* Expression**



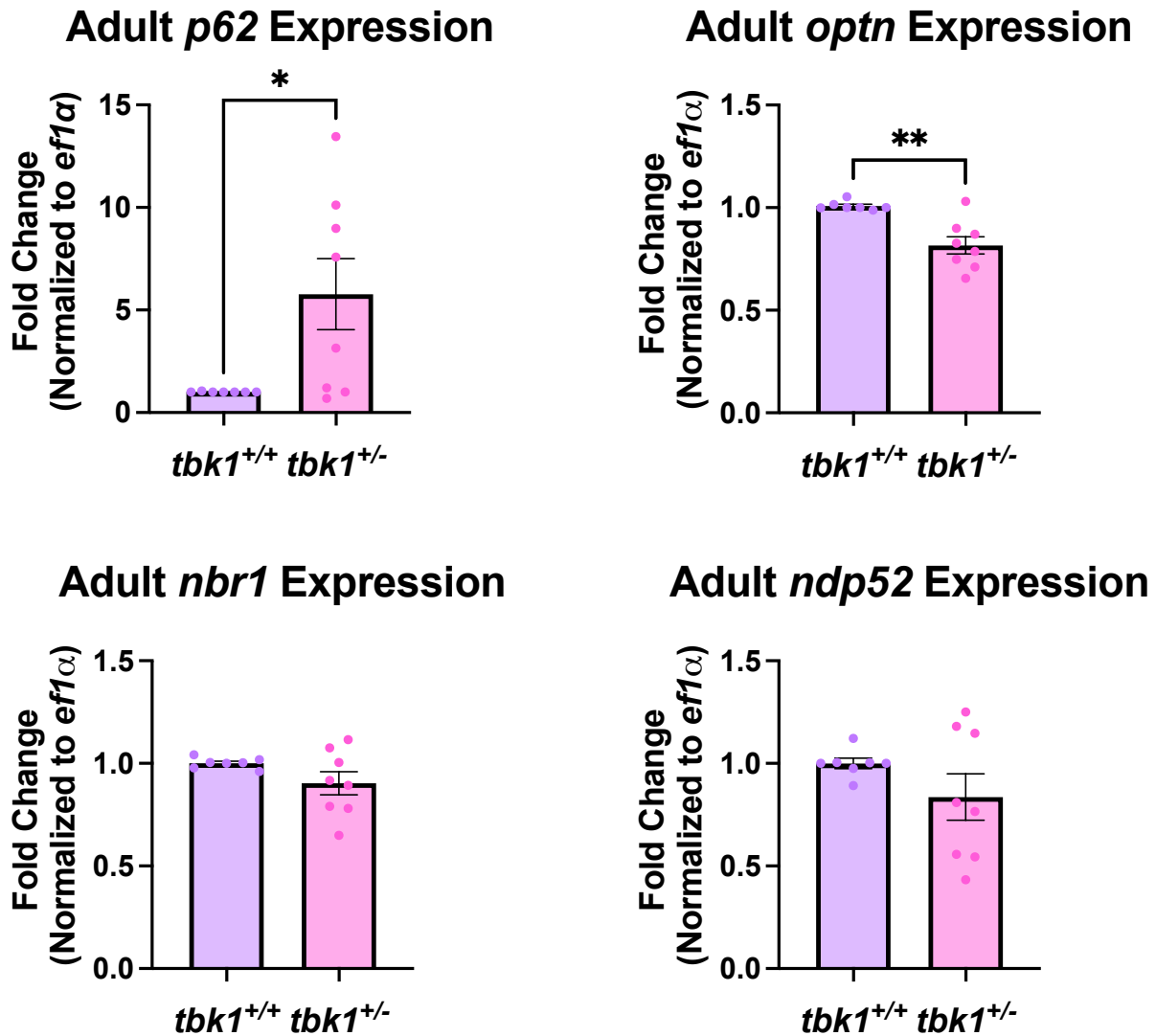


**Figure 11** | RT-qPCR analysis of known inflammatory markers involved in the Tbk1 signaling pathway in 1.5-year-old WT and *tbk1*<sup>+/-</sup> zebrafish. RNA was extracted from adult brains using the Applied Biosystems PicoPure RNA Isolation Kit (Fisher Scientific) and analyzed through unpaired t-test or Mann-Whitney test if data was not normally distributed. Significantly altered genes are as follows: for *tbk1*,  $U = 0$ ,  $p = 0.0003$ . For *irf3*,  $U = 3$ ,  $p = 0.002$ . For *irf7*,  $t(13) = 4.45$ ,  $p = 0.0007$ . For *p62*,  $U = 10$ ,  $p = 0.04$ . For *optn*,  $U = 6$ ,  $p = 0.009$ . For *ripk1*,  $t(13) = 3.70$ ,  $p = 0.003$ . For *il8*,  $t(13) = 4.57$ ,  $p = 0.0005$ . For *il10*,  $t(13) = 8.46$ ,  $p < 0.0001$ .  $n = 7$  for wild-type larvae and  $n = 8$  for heterozygous knockout larvae. (\*) indicates  $p < 0.05$ , (\*\*) indicates  $p < 0.01$ , (\*\*\*) indicates  $p < 0.001$ , (\*\*\*\*) indicates  $p < 0.0001$ .

### ***tbk1*<sup>+/-</sup> larvae display aberrant immune responses following LPS stimulation at 2 dpf**

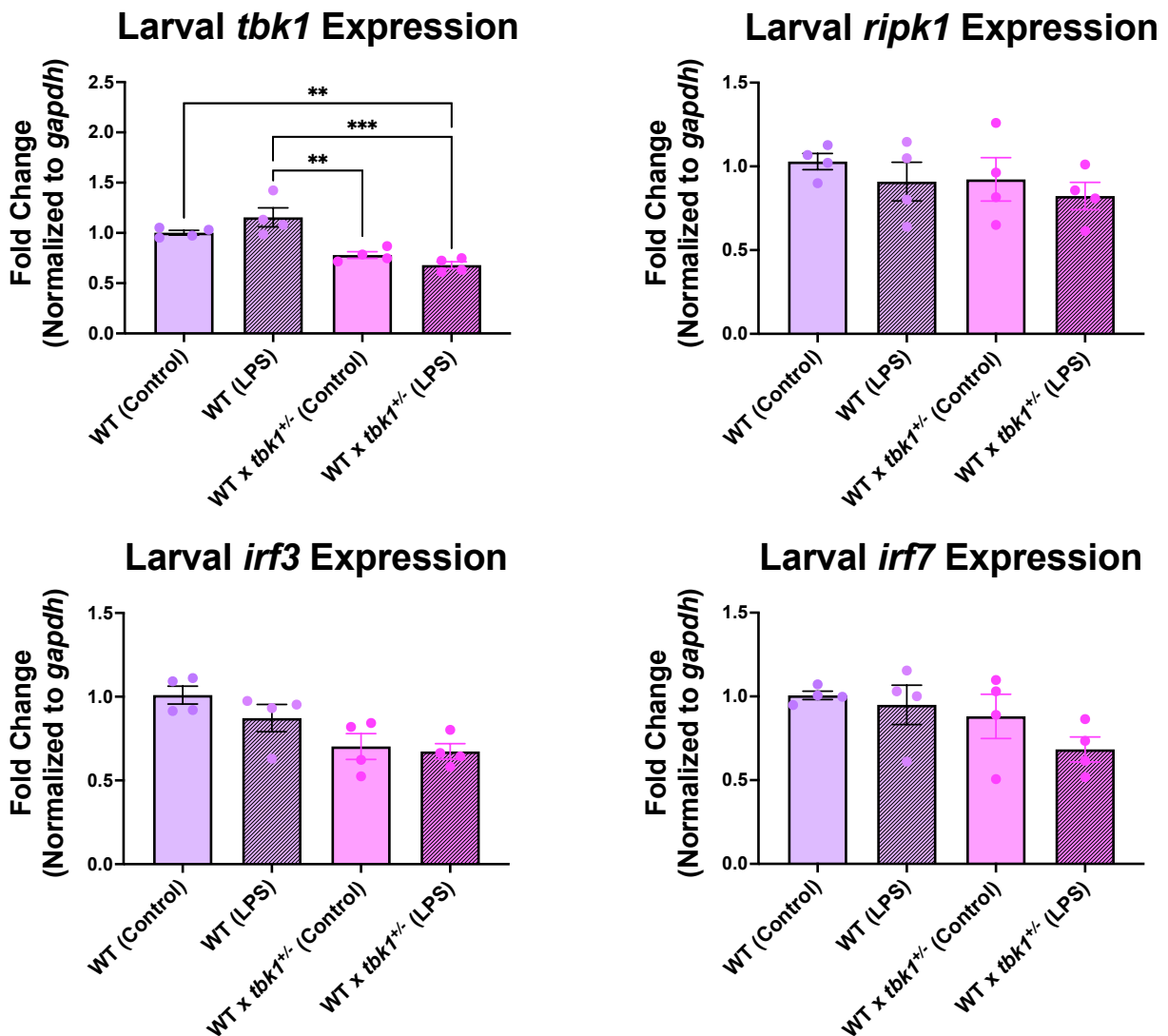
In light of the modest transcriptional alterations observed in the heterozygous *tbk1* KO zebrafish compared to WT counterparts, an experimental paradigm was designed to scrutinize the ramifications of diminished *tbk1* expression during an active immune response. To this end, an immune challenge was imposed on heterozygous KO zebrafish larvae, utilizing lipopolysaccharides (LPS) as an immune stressor. Notably, LPS, owing to its water solubility, was administered via a sublethal dosage (50 µg/mL) for a duration of 2 hours, with both WT and WT x *tbk1*<sup>+/-</sup> zebrafish larvae being subjected to this regimen. Subsequently, larvae of each genotype were amalgamated to facilitate RNA extraction for downstream analyses.

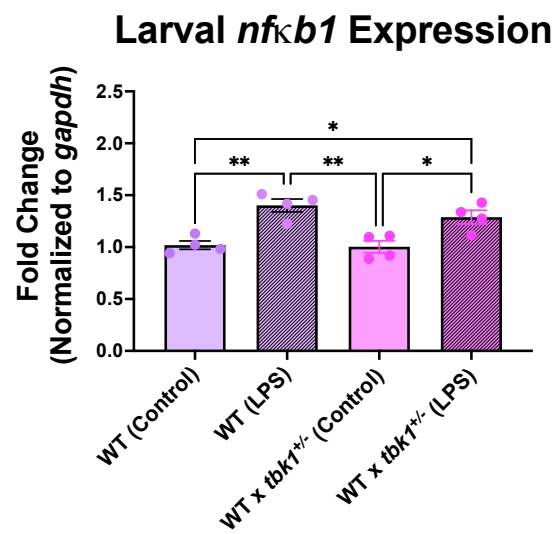
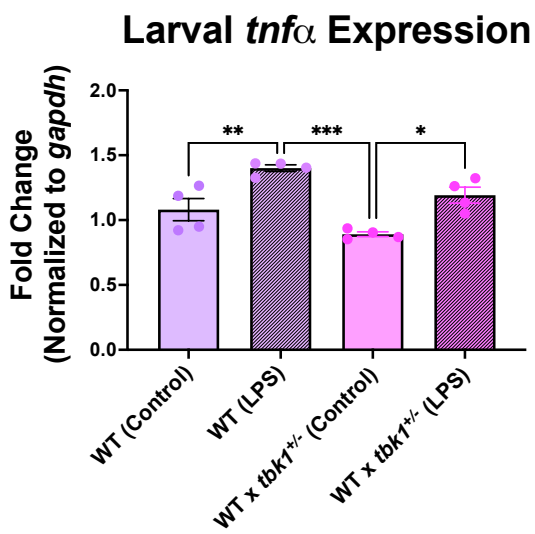
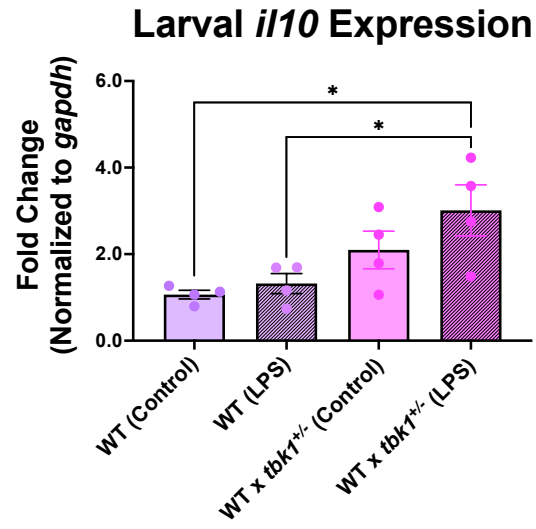
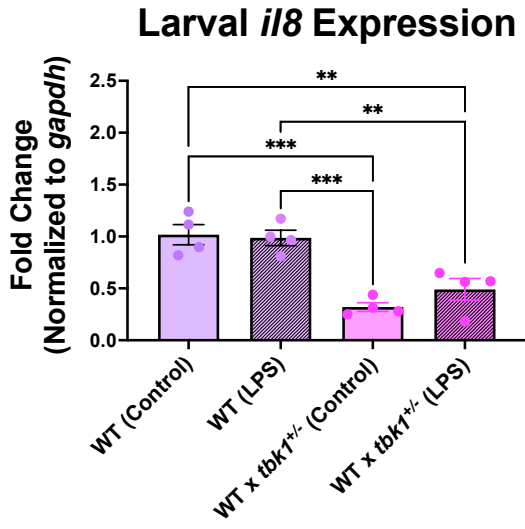
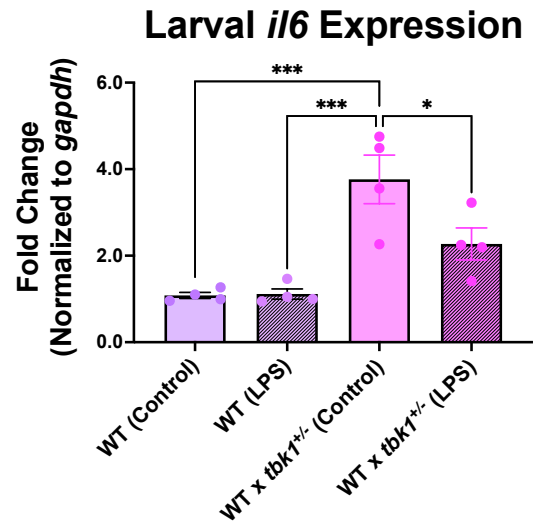
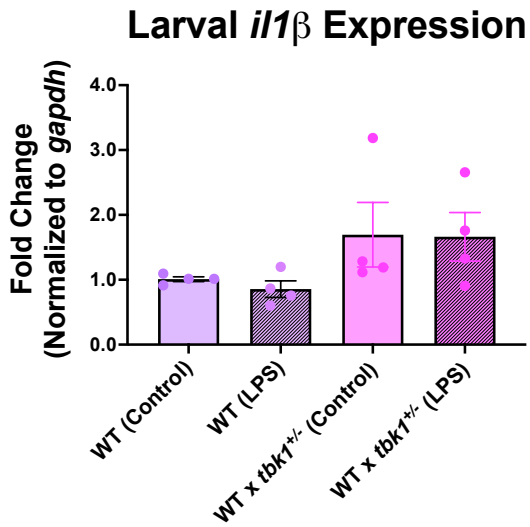
Genotyping zebrafish at this developmental juncture necessitates the sacrifice of the subjects. Thus, a cohort stemming from a WT x *tbk1*<sup>+/-</sup> cross was collated, adhering to Mendelian ratios yielding a 1:1 ratio of WT (*tbk1*<sup>+/+</sup>) and heterozygous (*tbk1*<sup>+/-</sup>) individuals. RT-qPCR was then employed to scrutinize alterations in the transcript levels of pertinent inflammatory markers associated with the Tbk1 signaling pathway, both in response to genotype variance and LPS treatment.

Evaluation of the transcriptional consequences ensuing from heterozygous *tbk1* ablation under immune stimulation was conducted through the immersion of both wild-type and WT x *tbk1*<sup>+/-</sup> pooled larvae (30 larvae) in LPS-treated system water. Crucially, it was observed that the presence of LPS did not modulate *tbk1* transcript levels when contrasted with control larvae (pooled wild type larvae). Upon comparing transcripts of interest contingent upon genotype, discernible alterations were noted: *p62* and *il6* exhibited upregulation, while *il8* and *ndp52* displayed downregulation in the pooled WT x *tbk1*<sup>+/-</sup> zebrafish larvae (**Figure 12**). Intriguingly, the comparison of this larval dataset with adult brain expression data (**Figure 11**) suggested that

the downregulation of *il8* and upregulation of *p62* constitute conserved consequences of heterozygous *tbk1* loss throughout developmental stages and adulthood.

Furthermore, it was observed that both *tnfa* and *nfkB* exhibited elevated expression levels in response to LPS administration in both wild-type and heterozygous knockout larvae. In contrast, *il6* displayed decreased expression levels in response to LPS administration in the WT x *tbk1*<sup>+/-</sup> larvae (**Figure 12**). This underscores the interplay between the Tbk1 signaling pathway and the transcriptional regulation of key inflammatory mediators in zebrafish larvae under immune stress conditions.





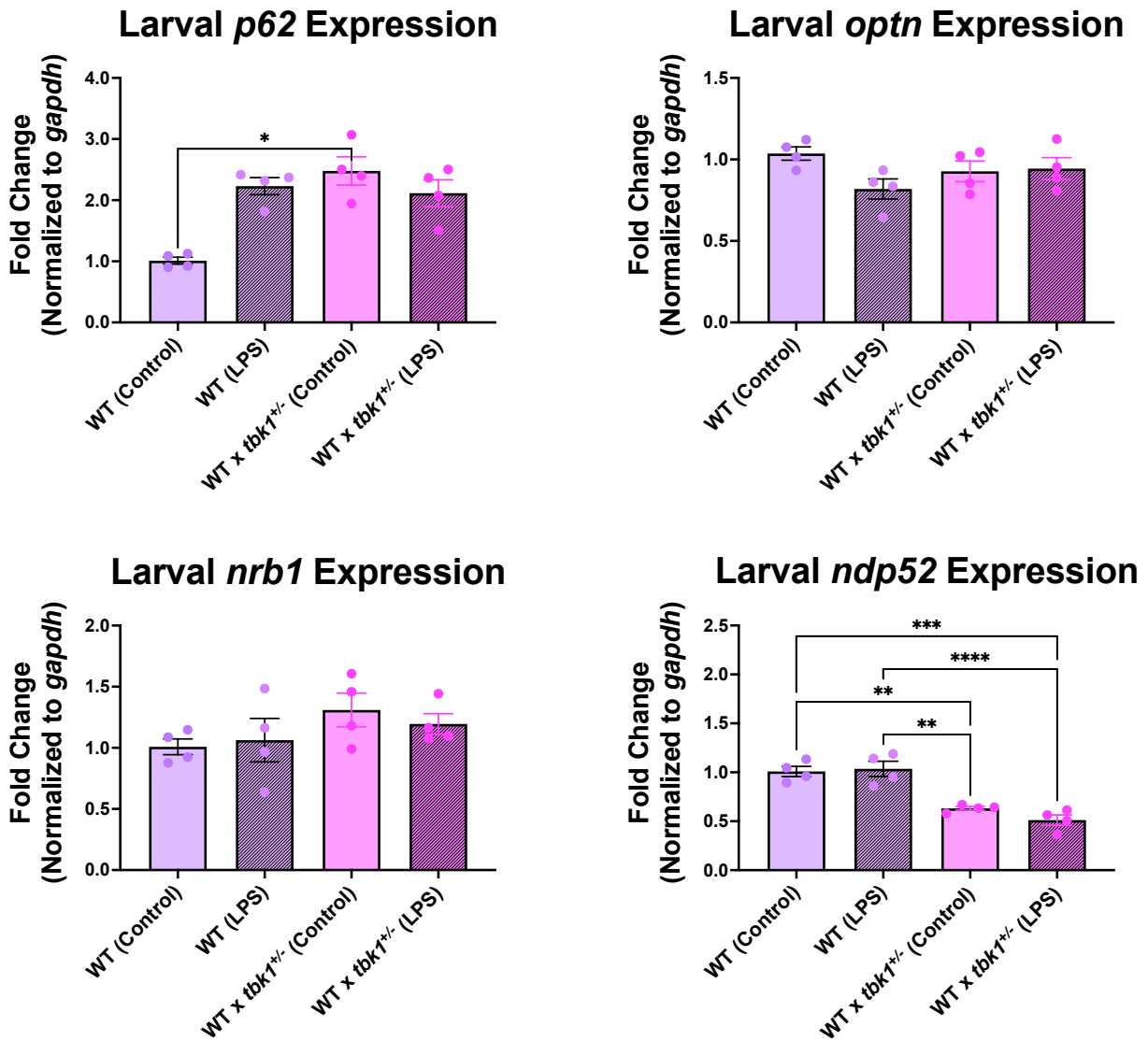


**Figure 12** | Transcriptional changes of immune-related genes in pooled larvae (2 dpf) from a heterozygous *tbk1*<sup>+/-</sup> crossed with wild type in response to immune challenge with LPS. Notably, upregulation of *p62* and *il6* alongside downregulation of *il8* and *ndp52* are observed in in pooled larvae compared to wild type, highlighting the impact of *tbk1* haploinsufficiency on immune response regulation. Additionally, both *tnfα* and *nfκb* exhibit heightened expression levels in response to LPS administration across genotypes, emphasizing the intricate interplay between the Tbk1 pathway and inflammatory transcriptional regulation. Significantly changed transcripts are as follows: For *tbk1*,  $F(3, 12) = 15.80$ ,  $p = 0.0002$ . For *irf3*, Kruskal-Wallis statistic = 8.49,  $p = 0.02$ , with no changes observed in subsequent multiple comparisons test. For *p62*, Kruskal-Wallis statistic = 9.55,  $p = 0.008$ . For *illb*, Kruskal-Wallis statistic = 7.36,  $p = 0.05$ ,

with no changes observed in subsequent multiple comparisons test. For *il6*,  $F(3, 12) = 13.59$ ,  $p = 0.0004$ . For *il8*,  $F(3, 12) = 17.96$ ,  $p < 0.0001$ . For *il10*,  $F(3, 12) = 5.10$ ,  $p = 0.02$ . For *tnfa*,  $F(3, 12) = 14.98$ ,  $p = 0.0002$ . For *nfkb*,  $F(3, 12) = 11.92$ ,  $p = 0.0007$ . For *ndp52*,  $F(3, 12) = 23.52$ ,  $p < 0.0001$ . Significance is indicated on the graphs above as follows: (\*) indicates  $p < 0.05$ , (\*\*) indicates  $p < 0.01$ , (\*\*\*) indicates  $p < 0.001$ , (\*\*\*\*) indicates  $p < 0.0001$ .

#### 4. Discussion

ALS is a multifactorial disease characterized by an intricate interplay of environmental, genetic, and molecular factors that despite intensive research efforts remains poorly understood (Peters et al., 2015). The recent identification of *TBK1* mutations in ALS patients has prompted further investigation into its role in diseases. Mutations in the *TBK1* gene manifest as nonsense, frameshift, missense, and deletion mutations, with nonsense and frameshift mutations that are believed to cause disease by TBK1 haploinsufficiency (Cirulli et al., 2015; Freischmidt et al., 2015). In the context of TBK1, research has highlighted its critical role in various cellular processes, including inflammation, autophagy, and immune response regulation (Oakes et al., 2017). Mutations leading to TBK1 haploinsufficiency disrupt these processes, contributing to the pathogenesis of ALS. The aim of this thesis was to characterize and determine a possible neurological phenotype in heterozygous (*tbk1*<sup>+/-</sup>) and homozygous (*tbk1*<sup>-/-</sup>) knockout zebrafish.

Zebrafish have emerged as a powerful model organism for studying vertebrate development and disease due to their high fecundity, external fertilization, and optical transparency during early embryogenesis (Babin et al., 2014; Howe et al., 2013). Utilizing zebrafish models in conjunction with CRISPR/Cas9 technology facilitates the *in vivo* investigation of gene function, providing valuable insights into the genetic basis of human diseases (Babin et al., 2014). Recent advances in zebrafish research have demonstrated their utility in modeling neurodegenerative diseases, including ALS. For example, studies have shown that zebrafish models can effectively recapitulate key aspects of ALS pathology, including motor neuron degeneration and protein aggregation (Armstrong & Drapeau, 2013; Babin et al., 2014; Roussel et al., 2021).

In this study, a zebrafish knockout line targeting the *tbk1* gene was generated using CRISPR/Cas9-mediated gene editing. The introduction of a single nucleotide deletion within exon 11 effectively induced multiple premature stop codons in the *tbk1* transcript, analogous to a mutation observed in an ALS patient from the Montreal Neurological Institute. This mutation was successfully transmitted to subsequent generations, enabling the generation of homozygous *tbk1* knockout (*tbk1*<sup>-/-</sup>) zebrafish through in-crossing of F1 offspring.

The nonsense mutation within the *tbk1* gene led to a significant reduction in *tbk1* expression levels in both adult and 5 dpf larval zebrafish heterozygous models. This reduction aligns with the cellular response to nonsense mutations, wherein aberrant transcripts containing premature stop codons are subjected to nonsense-mediated decay (NMD) (Kurosaki & Maquat, 2016). The observed decrease in *tbk1* expression underscores the effectiveness of the NMD pathway in mitigating the production of truncated and potentially deleterious proteins. This finding underscores the crucial role of TBK1 in maintaining cellular homeostasis and emphasizes the gene's functional importance in zebrafish development and physiology. Despite these findings, the challenge of obtaining a zebrafish-specific Tbk1 antibody persists. Approximately one-third of zebrafish antibodies fail to perform effectively (Bradford et al., 2022), complicating direct quantification of Tbk1 protein expression levels. To address this limitation, alternative approaches, such as mass spectrometry or other advanced proteomic techniques, are necessary. These methods would provide a more accurate assessment of Tbk1 protein abundance and function, thereby corroborating the observed reduction in *tbk1* expression at the protein level.

Previous research using murine models has demonstrated embryonic lethality in homozygous *Tbk1* knockout mice by E14.5, emphasizing the indispensable role of Tbk1 in vertebrate development (Bonnard et al., 2000; Hemmi et al., 2004). The external fertilization of

zebrafish eggs provided an advantage in assessing the consequences of homozygous *tbk1* loss on molecular pathways prior to death. In agreement with the findings of murine of *Tbk1* knockout murine models, homozygous *tbk1*<sup>-/-</sup> zebrafish exhibit a severely compromised lifespan, with individuals failing to survive beyond 15 dpf. This severe phenotype underscores the essential role of TBK1 in early development and highlights the catastrophic consequences of *tbk1* loss-of-function mutations. Furthermore, the evolutionary conservation of TBK1 function is further supported by the similarity of phenotypes observed in *tbk1* knockout models across different species. The lethality observed in both murine and zebrafish models suggests that *Tbk1*'s role in critical developmental and cellular processes is highly conserved.

The characterization of larval motor phenotypes in both heterozygous and homozygous *tbk1* KO zebrafish revealed significant alterations in burst swimming patterns at 2 dpf. Notably, the *tbk1*<sup>-/-</sup> zebrafish exhibited an unexpected increase in swim duration in touch-response assays. This finding contrasts with typical expectations for a knockout model of an ALS-associated gene, where decreased locomotor function is usually observed (Cirulli et al., 2015; Renton et al., 2011). To explore the underlying cause of this hyperactive phenotype, we investigated potential abnormalities in the NMJs of the zebrafish. Our analysis indicated reduced colocalization of pre- and post-synaptic markers at the NMJs, suggesting significant synaptic disruption at this site. This highlights the crucial role of TBK1 in maintaining NMJ integrity, aligning with previous studies that have implicated *TBK1* mutations resulting in impaired synaptic connectivity and motor neuron pathology (W. Duan et al., 2019; Freischmidt et al., 2015). Given the pronounced NMJ abnormalities, one would anticipate a corresponding decrease in motor function in the homozygous *tbk1* KO zebrafish at 2 dpf. However, the observed increase in swim duration points to a complex interplay of factors influencing motor behaviour. At this developmental stage,

zebrafish burst swimming patterns are predominantly driven by the depolarization of neuronal membrane potential driven by an embryonically reversed chloride ion gradient. It is plausible that the homozygous loss of *tbk1* influences chloride ion dynamics, leading to the observed hyperactive phenotype. Further investigation into the role of chloride in this context is warranted. Utilizing chloride-sensitive dyes, such as MQAE (N-(ethoxycarbonylmethyl)-6-methoxyquinolinium bromide), could provide insights into chloride ion concentration differences in motor neurons and its impact on zebrafish burst swimming patterns. This would enhance our understanding of the molecular underpinnings of motor function abnormalities in *tbk1* KO models and potentially uncover novel therapeutic targets for ALS and related motor neuron diseases.

During early development, zebrafish exhibit a burst swimming pattern (Buss & Drapeau, 2001), which gradually transitions to a beat-and-glide pattern as their NMJs and motor circuits mature (Roussel et al., 2021; Saint-Amant & Drapeau, 2000). Subsequent motor function analysis at 8 dpf demonstrated a marked reduction in mean swim velocity in the *tbk1*<sup>-/-</sup> larvae. At this developmental stage, zebrafish locomotor systems have matured, resulting in the fish developing a beat-and-glide swimming pattern. This observed shift from a hyperactive motor phenotype at 2 dpf to a hypoactive motor phenotype at 8 dpf may be attributed to the maturation of the neuronal systems controlling locomotion. Another possibility for this observed shift is related to the viability of the homozygous *tbk1* KO zebrafish. Our analysis revealed an initial decrease in the presence of homozygous *tbk1* knockout (KO) zebrafish between 5 and 10 dpf, shifting from 15% to 8% in the Mendelian ratio. This reduction could suggest a potential selective disadvantage or increased mortality rate in *tbk1*<sup>-/-</sup> larvae during this period. Recent studies have shown that TBK1 plays a crucial role in various cellular processes, including

inflammation and autophagy (Oakes et al., 2017). The loss of TBK1 function could lead to dysregulation in these processes, contributing to the decreased viability and altered motor phenotypes observed. To further elucidate the underlying mechanisms of these motor phenotypes, a detailed analysis of NMJ development and function in *tbk1*<sup>-/-</sup> zebrafish larvae is warranted. Performing an NMJ colocalization analysis on 8 dpf larvae and comparing it with 2 dpf larvae could provide insights into the maturation and functionality of NMJs in the absence of Tbk1. This analysis could reveal potential defects in NMJ structure or function that contribute to the hypoactive motor phenotype at later stages of development.

Given that ALS typically manifests as a late adult-onset disease, our investigation was extended to evaluate locomotor function in adult 1.5-year-old wild-type and *tbk1*<sup>+/-</sup> zebrafish. Remarkably, the analysis revealed no significant differences in locomotor performance between the wild-type and heterozygous zebrafish at this age. The lack of significant locomotor deficits in the heterozygous *tbk1* zebrafish could be attributed to several factors. Firstly, the deletion of a single *tbk1* allele may not be sufficient to induce a discernible motor phenotype in adult zebrafish, which might be due to compensatory mechanisms. In zebrafish, as in other organisms, genetic redundancy and compensation by other pathways can mitigate the impact of single-gene mutations (El-Brolosy & Stainier, 2017). Moreover, the absence of motor deficits in 1.5-year-old zebrafish, technically classified as young adults, aligns with the understanding that ALS is a progressive neurodegenerative disease typically presenting clinical symptoms in later stages of life. This timing suggests that additional genetic or environmental factors may be necessary to fully manifest the motor deficits associated with ALS. For example, research has demonstrated that environmental stressors or additional genetic mutations can exacerbate the onset and progression of neurodegenerative diseases, suggesting a multifactorial aetiology for conditions

like ALS (Peters et al., 2015). Future studies should consider extending the age range of the zebrafish model to older stages, closer to the equivalent human late adulthood, to determine if the motor deficits appear later in life. Additionally, examining the interplay between *tbk1* haploinsufficiency and other ALS-associated genetic or environmental factors could provide deeper insights into the pathogenesis of the disease.

The *TBK1* gene is recognized as the first ALS-associated gene directly implicated in neuroinflammatory pathways. To elucidate its role in neuroinflammation, an RT-qPCR analysis was conducted on genes involved in neuroinflammation and autophagy within the Tbk1 signaling pathway in adult zebrafish aged 1.5 years. This transcriptional analysis revealed significant alterations in gene expression in heterozygous *tbk1* KO adult zebrafish. Notably, there was a significant upregulation in the expression of Tbk1's immediate downstream targets, *irf3* and *irf7*. Since 1.5-year-old zebrafish are considered young adults, it is possible that the full impact of heterozygous *tbk1* KO on ALS phenotype manifestation might not yet be observable, as ALS is typically a late-onset disease. The observed upregulation of *irf3* and *irf7* suggests a compensatory mechanism for the reduced *tbk1* expression, potentially explaining the absence of an ALS-like phenotype at this developmental stage.

Additionally, we observed an upregulation of *p62* (*sqstm1*), the transcript encoding the autophagy cargo protein p62, in *tbk1*<sup>+/-</sup> zebrafish. This protein is known to colocalize with cytoplasmic inclusions in ALS patients, indicating proteostasis defects (Blokhuys et al., 2013; Gal, Strom, Kilty, Zhang, & Zhu, 2007). The role of p62/SQSTM1 in ALS pathology has been further substantiated by recent findings that link p62 to the degradation of ubiquitinated protein aggregates via autophagy. Therefore, the increased expression of *p62* might signify the early stages of an ALS-like phenotype.

Conversely, a downregulation of *optn* was noted in *tbk1*<sup>+/-</sup> zebrafish. TBK1's role in recycling protein aggregates is mediated through the phosphorylation of the autophagy receptor optineurin (Optn). TBK1 has been reported to colocalize with Optn and cellular aggregates in HeLa cells in vitro, as well as in a SOD1 transgenic mouse model of ALS (Moore & Holzbaur, 2016). Thus, reduced *tbk1* expression could directly result in decreased *optn* expression, affecting the cellular autophagy mechanisms.

Furthermore, we detected a slight downregulation of *ripk1* in the *tbk1*<sup>+/-</sup> zebrafish. Xu et al. (2018) demonstrated that TAK1, a kinase regulator of RIPK1, exhibits decreased expression in the aging human brain, potentially increasing the brain's sensitivity to TBK1 dysregulation and linking it to the late onset of ALS. Although the reduction in *ripk1* expression was statistically significant, the slight magnitude raises questions about the robustness of this finding.

Finally, heterozygous *tbk1* KO zebrafish exhibit a significant decrease in both *il8* and *il10* expression. IL-8, a chemokine secreted by macrophages, plays a crucial role in the recruitment of neutrophils to sites of inflammation. TBK1 typically upregulates *il8* expression by activating NF- $\kappa$ B and other transcription factors involved in pro-inflammatory responses (Ahmad et al., 2016; Runde, Mack, S, & Zhang, 2022). Therefore, the observed decrease in *il8* expression is consistent with the reduced *tbk1* expression. However, our analysis shows no differences in the expression of *nfk1* between the wild-type and *tbk1*<sup>+/-</sup> zebrafish. This finding suggests that the decreased expression of *il8* at 1.5 years of age may be attributed to the complex downstream molecular pathways influenced by TBK1, beyond the activation of NF- $\kappa$ B. TBK1 is known to phosphorylate various substrates involved in immune signaling, indicating a multi-faceted role in cytokine regulation (S. Liu et al., 2015; Peters et al., 2015).

The observed decrease in *il10* expression in response to decreased *tbk1* expression underscores the complexity of immune regulation. IL-10 is an anti-inflammatory cytokine that enhances B-cell survival and proliferation, as well as suppressing excessive inflammatory responses (Carlini et al., 2023). TBK1's role in *il10* expression appears more nuanced than *il8*, often acting to suppress it by promoting a pro-inflammatory state. This suppression can vary depending on the specific cellular context and the presence of other regulatory factors (Clark et al., 2012; Mittal & Roche, 2015). Therefore, a decrease in *tbk1* expression should result in an increase in *il10* expression. This paradox observed suggests a complex regulatory network involving Tbk1. TBK1 interacts with various signaling proteins, such as the IRF family, crucial for immune response modulation. Reduced TBK1 activity disrupts these interactions, possibly affecting transcription factors that TBK1 modulates. Moreover, TBK1's role includes signaling crosstalk and compensatory mechanisms, which might adjust to maintain immune homeostasis, inadvertently reducing *il10* expression levels. The presence of complex feedback loops could also lead to unexpected cytokine expression patterns when TBK1 is altered.

Interestingly, transcriptional alterations in the pro-inflammatory cytokines IL-1 $\beta$ , IL-6, and TNF $\alpha$ , were not observed at this developmental stage. This absence of change suggests that the modulation of *tbk1* does not universally affect all cytokines uniformly but rather exerts selective regulatory effects, potentially depending on the stage of development and specific cellular environments.

These findings underscore the intricate regulatory interplay between TBK1 and its downstream effectors involved in immune responses and cellular homeostasis. The reduction of *tbk1* expression disrupts normal immune functions, as evidenced by the inappropriate immune responses observed in zebrafish at this developmental age. This disruption highlights the critical

role of TBK1 in modulating immune signaling pathways and maintaining immune system equilibrium.

The modest transcriptional alterations in the adult heterozygous *tbk1* KO zebrafish led us to investigate the ramifications of diminished *tbk1* expression during an active immune response between 2 dpf wild-type and offspring of a WT x *tbk1*<sup>+/-</sup> cross. The effect of genotype and the effect of treatment were both assessed in this analysis. Regarding the effect of genotype, *p62* and *il6* exhibited upregulation, while *il8* and *ndp52* displayed downregulation in the WT x heterozygous knockouts. Intriguingly, comparison of this larval dataset with adult brain expression data, elucidated that downregulation of *il8* and upregulation of *p62* constitute conserved consequences of heterozygous *tbk1* loss throughout developmental stages and adulthood. The upregulation of *p62* observed in our study aligns with findings that TBK1 is crucial for autophagic clearance, where p62 serves as a key adaptor protein in autophagy (Oakes et al., 2017). The increased expression of *p62* may reflect a compensatory mechanism in response to impaired TBK1 function, aimed at maintaining autophagic flux at this developmental stage. The upregulation of *il6* and downregulation of *il8* in WT x heterozygous *tbk1* zebrafish larvae further underscore the nuanced role of TBK1 in immune responses. IL-6 is a multifunctional cytokine involved in inflammation and tissue regeneration (Yu et al., 2012), and its upregulation might indicate an attempt to counteract immune dysregulation caused by TBK1 insufficiency. Conversely, the downregulation of *il8* suggests a compromised inflammatory response, which could have implications for the organism's ability to combat infections effectively.

Moreover, the downregulation of *ndp52*, another autophagy-related gene, in WT x heterozygous *tbk1* larvae, supports the notion of compromised autophagic processes in the

absence of full Tbk1 activity. NDP52 is involved in recognizing and targeting ubiquitinated pathogens for autophagic degradation (Vargas et al., 2019), and its decreased expression could signify a reduced capacity for pathogen clearance.

Regarding the effect of LPS treatment, significant transcriptional alterations were observed. Notably, *tbk1* expression remained unchanged upon LPS exposure in both wild-type (WT) and WT x heterozygous *tbk1* genotypes. In contrast, both *tnfa* and *nfkb1* exhibited significantly elevated expression levels following LPS administration in both WT and heterozygous knockout larvae. This observation corroborates with existing literature that demonstrates the upregulation of *TNF $\alpha$*  and *NF- $\kappa$ B* in response to LPS, highlighting their critical roles in mediating inflammatory responses (Hobbs, Reynoso, Geddis, Mitrophanov, & Matheny, 2018; Reis et al., 2011). Interestingly, *il6* expression was found to be decreased in response to LPS in WT x *tbk1*<sup>+/-</sup> larvae. It is noteworthy that the baseline transcription levels of *il6* were already elevated in these larvae, suggesting a possible negative feedback mechanism. The initial high expression levels of *il6* may have triggered an immune response that subsequently led to its decreased expression upon further immune stimulation. This finding underscores the complex interplay between the TBK1 signaling pathway and the transcriptional regulation of key inflammatory mediators under immune stress conditions. The study's results indicate that despite the presence of a cohort of WT x heterozygous zebrafish larvae, significant differences in expression levels were evident. This suggests that the heterozygous state of *tbk1* can profoundly influence the inflammatory response, even in a mixed genotype population.

Our preliminary characterization of a zebrafish *tbk1* knockout (KO) model has revealed phenotypes that are consistent with those observed in mouse *tbk1* KOs and those associated with ALS pathophysiology. This zebrafish *tbk1* KO model presents significant potential for future

drug screening, offering a unique opportunity to evaluate water-soluble compounds directly in the aquatic environment of the fish (Bradford et al., 2022; Howe et al., 2013). This feature allows for efficient and high-throughput screening of potential therapeutic compounds. Furthermore, the transparency of zebrafish embryos facilitates real-time observation of phenotypic changes and drug effects, making them a powerful model for studying gene-environment interactions and compound efficacy (Bradford et al., 2022; Howe et al., 2013). Recent research has highlighted the crucial role of TBK1 in ALS, particularly in the regulation of neuroinflammation and autophagy. Mutations in TBK1 are known to impair its kinase activity, leading to dysregulation of these critical cellular processes (Freischmidt et al., 2015). By using the zebrafish *tbk1* KO model, we can delve deeper into the molecular mechanisms underpinning TBK1-related ALS pathogenesis. This model enables the identification of novel drug targets and the evaluation of compound efficacy in a whole-organism context. We propose leveraging this model with sublethal LPS treatment to conduct chemical screens aimed at identifying compounds capable of restoring the expression of misregulated genes. LPS treatment can induce a controlled inflammatory response, mimicking aspects of the neuroinflammatory environment observed in ALS. This approach will allow us to assess the therapeutic potential of compounds in modulating gene expression and alleviating ALS-related phenotypes. In conclusion, our zebrafish *tbk1* KO model is a promising tool for ALS research and drug discovery. It offers a robust platform for high-throughput screening and detailed investigation of TBK1-associated pathways. Future studies utilizing this model could lead to significant advancements in our understanding of ALS and the development of effective therapies.

## **5. Conclusion**

This thesis presents an insightful exploration into the role of TANK-Binding Kinase 1 (TBK1) in the pathogenesis of ALS through a zebrafish model. The study successfully established a *tbk1* knockout model using the CRISPR/Cas9 genome editing system, providing a robust platform to elucidate the functional impacts of TBK1 deficiency in a vertebrate model. The findings demonstrate that *tbk1* knockout zebrafish exhibit ALS-like phenotypes, including significant motor dysfunction and neuroinflammation, paralleling human disease manifestations. The initial characterization of *tbk1*<sup>-/-</sup> zebrafish larvae revealed a striking inability to survive beyond 15 dpf, underscored by early hyperactivity followed by severe motor impairment. This rapid decline in motor function and survival highlights the critical role of TBK1 in maintaining neuromuscular integrity. Immunofluorescence analysis further confirmed synaptic defects at the NMJ, as evidenced by the increased presence of orphaned pre- and post-synaptic markers in *tbk1*<sup>-/-</sup> larvae compared to the WT and *tbk1*<sup>+/-</sup> larvae. In adult *tbk1*<sup>+/-</sup> zebrafish, the absence of a discernible motor phenotype at 1.5 years of age suggests that heterozygous loss of *tbk1* may not be sufficient to trigger overt motor deficits within this timeframe. However, significant transcriptional dysregulation was observed, with upregulated expression of *irf3*, *irf7*, and *p62*, alongside downregulated expression of *optn*, *il8*, *il10*, and *ripk1*, indicating disrupted immune and autophagy responses due to decreased *tbk1* expression. These molecular changes align with known ALS pathology, underscoring TBK1's role in disease mechanisms. The study also evaluated the impact of immune challenges on Tbk1 signaling by exposing zebrafish larvae to LPS. Notably, LPS exposure induced significant transcriptional changes in inflammatory and autophagy-related genes, including the upregulation of *p62* and *il6* and downregulation of *il8* and *ndp52* in WT x *tbk1*<sup>+/-</sup> offspring. This indicates a complex interplay between TBK1 and immune

response modulation under stress conditions. The consistent downregulation of *il8* and upregulation of *p62* across developmental stages further emphasizes TBK1's involvement in immune regulation. The findings from this research advance our understanding of ALS pathogenesis by highlighting the critical involvement of TBK1 in neuroinflammation and autophagy dysregulation. This zebrafish model provides a valuable tool for future studies aimed at exploring therapeutic strategies targeting TBK1 pathways. By elucidating the molecular underpinnings of TBK1's role in ALS, this work paves the way for innovative approaches to combat this devastating neurodegenerative disease.

## 6. Preliminary Bibliography

- Ahmad, L., Zhang, S. Y., Casanova, J. L., & Sancho-Shimizu, V. (2016). Human TBK1: A Gatekeeper of Neuroinflammation. *Trends Mol Med*, 22(6), 511-527. doi:10.1016/j.molmed.2016.04.006
- Amin, A., Perera, N. D., Beart, P. M., Turner, B. J., & Shabanpoor, F. (2020). Amyotrophic Lateral Sclerosis and Autophagy: Dysfunction and Therapeutic Targeting. *Cells*, 9(11). doi:10.3390/cells9112413
- Armstrong, G. A., & Drapeau, P. (2013). Loss and gain of FUS function impair neuromuscular synaptic transmission in a genetic model of ALS. *Hum Mol Genet*, 22(21), 4282-4292. doi:10.1093/hmg/ddt278
- Armstrong, G. A., Liao, M., You, Z., Lissouba, A., Chen, B. E., & Drapeau, P. (2016). Homology Directed Knockin of Point Mutations in the Zebrafish *tardbp* and *fus* Genes in ALS Using the CRISPR/Cas9 System. *PLoS One*, 11(3), e0150188. doi:10.1371/journal.pone.0150188
- Babin, P. J., Goizet, C., & Raldua, D. (2014). Zebrafish models of human motor neuron diseases: advantages and limitations. *Prog Neurobiol*, 118, 36-58. doi:10.1016/j.pneurobio.2014.03.001
- Blokhuys, A. M., Groen, E. J., Koppers, M., van den Berg, L. H., & Pasterkamp, R. J. (2013). Protein aggregation in amyotrophic lateral sclerosis. *Acta Neuropathol*, 125(6), 777-794. doi:10.1007/s00401-013-1125-6
- Bonnard, M., Mirtsos, C., Suzuki, S., Graham, K., Huang, J., Ng, M., . . . Yeh, W. C. (2000). Deficiency of T2K leads to apoptotic liver degeneration and impaired NF-kappaB-dependent gene transcription. *EMBO J*, 19(18), 4976-4985. doi:10.1093/emboj/19.18.4976
- Bose, P., Armstrong, G. A. B., & Drapeau, P. (2019). Neuromuscular junction abnormalities in a zebrafish loss-of-function model of TDP-43. *J Neurophysiol*, 121(1), 285-297. doi:10.1152/jn.00265.2018
- Bradford, Y. M., Van Slyke, C. E., Ruzicka, L., Singer, A., Eagle, A., Fashena, D., . . . Westerfield, M. (2022). Zebrafish information network, the knowledgebase for *Danio rerio* research. *Genetics*, 220(4). doi:10.1093/genetics/iyac016
- Brenner, D., Sieverding, K., Bruno, C., Luningschror, P., Buck, E., Mungwa, S., . . . Weishaupt, J. H. (2019). Heterozygous *Tbk1* loss has opposing effects in early and late stages of ALS in mice. *J Exp Med*, 216(2), 267-278. doi:10.1084/jem.20180729
- Bright, F., Chan, G., van Hummel, A., Ittner, L. M., & Ke, Y. D. (2021). TDP-43 and Inflammation: Implications for Amyotrophic Lateral Sclerosis and Frontotemporal Dementia. *Int J Mol Sci*, 22(15). doi:10.3390/ijms22157781
- Brooks, B. R. (1994). El Escorial World Federation of Neurology criteria for the diagnosis of amyotrophic lateral sclerosis. Subcommittee on Motor Neuron Diseases/Amyotrophic Lateral Sclerosis of the World Federation of Neurology Research Group on Neuromuscular Diseases and the El Escorial "Clinical limits of amyotrophic lateral sclerosis" workshop contributors. *J Neurol Sci*, 124 Suppl, 96-107. doi:10.1016/0022-510x(94)90191-0
- Burgess, H. A., & Granato, M. (2007). Modulation of locomotor activity in larval zebrafish during light adaptation. *J Exp Biol*, 210(Pt 14), 2526-2539. doi:10.1242/jeb.003939

- Buss, R. R., & Drapeau, P. (2001). Synaptic Drive to Motoneurons During Fictive Swimming in the Developing Zebrafish. *Journal of Neurophysiology*, *86*(1), 197-210. Retrieved from <http://jn.physiology.org/content/86/1/197.abstract>
- Campanari, M. L., Garcia-Ayllon, M. S., Ciura, S., Saez-Valero, J., & Kabashi, E. (2016). Neuromuscular Junction Impairment in Amyotrophic Lateral Sclerosis: Reassessing the Role of Acetylcholinesterase. *Front Mol Neurosci*, *9*, 160. doi:10.3389/fnmol.2016.00160
- Carlini, V., Noonan, D. M., Abdalalem, E., Goletti, D., Sansone, C., Calabrone, L., & Albini, A. (2023). The multifaceted nature of IL-10: regulation, role in immunological homeostasis and its relevance to cancer, COVID-19 and post-COVID conditions. *Front Immunol*, *14*, 1161067. doi:10.3389/fimmu.2023.1161067
- Chen, Q., Sun, L., & Chen, Z. J. (2016). Regulation and function of the cGAS-STING pathway of cytosolic DNA sensing. *Nat Immunol*, *17*(10), 1142-1149. doi:10.1038/ni.3558
- Cirulli, E. T., Lasseigne, B. N., Petrovski, S., Sapp, P. C., Dion, P. A., Leblond, C. S., . . . Goldstein, D. B. (2015). Exome sequencing in amyotrophic lateral sclerosis identifies risk genes and pathways. *Science*, *347*(6229), 1436-1441. doi:10.1126/science.aaa3650
- Clark, K., MacKenzie, K. F., Petkevicius, K., Kristariyanto, Y., Zhang, J., Choi, H. G., . . . Cohen, P. (2012). Phosphorylation of CRT3 by the salt-inducible kinases controls the interconversion of classically activated and regulatory macrophages. *Proc Natl Acad Sci U S A*, *109*(42), 16986-16991. doi:10.1073/pnas.1215450109
- Clarke, B. E., & Patani, R. (2020). The microglial component of amyotrophic lateral sclerosis. *Brain*, *143*(12), 3526-3539. doi:10.1093/brain/awaa309
- DeJesus-Hernandez, M., Mackenzie, I. R., Boeve, B. F., Boxer, A. L., Baker, M., Rutherford, N. J., . . . Rademakers, R. (2011). Expanded GGGGCC hexanucleotide repeat in noncoding region of C9ORF72 causes chromosome 9p-linked FTD and ALS. *Neuron*, *72*(2), 245-256. doi:10.1016/j.neuron.2011.09.011
- Duan, Q. Q., Jiang, Z., Su, W. M., Gu, X. J., Wang, H., Cheng, Y. F., . . . Chen, Y. P. (2023). Risk factors of amyotrophic lateral sclerosis: a global meta-summary. *Front Neurosci*, *17*, 1177431. doi:10.3389/fnins.2023.1177431
- Duan, W., Guo, M., Yi, L., Zhang, J., Bi, Y., Liu, Y., . . . Li, C. (2019). Deletion of Tbk1 disrupts autophagy and reproduces behavioral and locomotor symptoms of FTD-ALS in mice. *Aging (Albany NY)*, *11*(8), 2457-2476. doi:10.18632/aging.101936
- El-Brolosy, M. A., & Stainier, D. Y. R. (2017). Genetic compensation: A phenomenon in search of mechanisms. *PLoS Genet*, *13*(7), e1006780. doi:10.1371/journal.pgen.1006780
- Fitzgerald, K. A., McWhirter, S. M., Faia, K. L., Rowe, D. C., Latz, E., Golenbock, D. T., . . . Maniatis, T. (2003). IKKepsilon and TBK1 are essential components of the IRF3 signaling pathway. *Nat Immunol*, *4*(5), 491-496. doi:10.1038/ni921
- Freischmidt, A., Wieland, T., Richter, B., Ruf, W., Schaeffer, V., Muller, K., . . . Weishaupt, J. H. (2015). Haploinsufficiency of TBK1 causes familial ALS and fronto-temporal dementia. *Nat Neurosci*, *18*(5), 631-636. doi:10.1038/nn.4000
- Gal, J., Strom, A. L., Kilty, R., Zhang, F., & Zhu, H. (2007). p62 accumulates and enhances aggregate formation in model systems of familial amyotrophic lateral sclerosis. *J Biol Chem*, *282*(15), 11068-11077. doi:10.1074/jbc.M608787200
- Garofalo, S., Coccozza, G., Bernardini, G., Savage, J., Raspa, M., Aronica, E., . . . Limatola, C. (2022). Blocking immune cell infiltration of the central nervous system to tame Neuroinflammation in Amyotrophic lateral sclerosis. *Brain Behav Immun*, *105*, 1-14. doi:10.1016/j.bbi.2022.06.004

- Gatica, D., Lahiri, V., & Klionsky, D. J. (2018). Cargo recognition and degradation by selective autophagy. *Nat Cell Biol*, 20(3), 233-242. doi:10.1038/s41556-018-0037-z
- Gatot, J. S., Gioia, R., Chau, T. L., Patrascu, F., Warnier, M., Close, P., . . . Chariot, A. (2007). Lipopolysaccharide-mediated interferon regulatory factor activation involves TBK1-IKKepsilon-dependent Lys(63)-linked polyubiquitination and phosphorylation of TANK/I-TRAF. *J Biol Chem*, 282(43), 31131-31146. doi:10.1074/jbc.M701690200
- Gerbino, V., Kaunga, E., Ye, J., Canzio, D., O'Keeffe, S., Rudnick, N. D., . . . Maniatis, T. (2020). The Loss of TBK1 Kinase Activity in Motor Neurons or in All Cell Types Differentially Impacts ALS Disease Progression in SOD1 Mice. *Neuron*, 106(5), 789-805 e785. doi:10.1016/j.neuron.2020.03.005
- Giorgi, C., Marchi, S., Simoes, I. C. M., Ren, Z., Morciano, G., Perrone, M., . . . Wieckowski, M. R. (2018). Mitochondria and Reactive Oxygen Species in Aging and Age-Related Diseases. *Int Rev Cell Mol Biol*, 340, 209-344. doi:10.1016/bs.ircmb.2018.05.006
- Goncalves, A., Burckstummer, T., Dixit, E., Scheicher, R., Gorna, M. W., Karayel, E., . . . Superti-Furga, G. (2011). Functional dissection of the TBK1 molecular network. *PLoS One*, 6(9), e23971. doi:10.1371/journal.pone.0023971
- Goyal, N. A., Berry, J. D., Windebank, A., Staff, N. P., Maragakis, N. J., van den Berg, L. H., . . . Cudkovicz, M. (2020). Addressing heterogeneity in amyotrophic lateral sclerosis CLINICAL TRIALS. *Muscle Nerve*, 62(2), 156-166. doi:10.1002/mus.26801
- Grosskreutz, J., Van Den Bosch, L., & Keller, B. U. (2010). Calcium dysregulation in amyotrophic lateral sclerosis. *Cell Calcium*, 47(2), 165-174. doi:10.1016/j.ceca.2009.12.002
- Hardiman, O., Al-Chalabi, A., Chio, A., Corr, E. M., Logroscino, G., Robberecht, W., . . . van den Berg, L. H. (2017). Amyotrophic lateral sclerosis. *Nat Rev Dis Primers*, 3, 17085. doi:10.1038/nrdp.2017.85
- Hemmi, H., Takeuchi, O., Sato, S., Yamamoto, M., Kaisho, T., Sanjo, H., . . . Akira, S. (2004). The roles of two IkappaB kinase-related kinases in lipopolysaccharide and double stranded RNA signaling and viral infection. *J Exp Med*, 199(12), 1641-1650. doi:10.1084/jem.20040520
- Heo, J. M., Ordureau, A., Paulo, J. A., Rinehart, J., & Harper, J. W. (2015). The PINK1-PARKIN Mitochondrial Ubiquitylation Pathway Drives a Program of OPTN/NDP52 Recruitment and TBK1 Activation to Promote Mitophagy. *Mol Cell*, 60(1), 7-20. doi:10.1016/j.molcel.2015.08.016
- Herhaus, L. (2021). TBK1 (TANK-binding kinase 1)-mediated regulation of autophagy in health and disease. *Matrix Biol*, 100-101, 84-98. doi:10.1016/j.matbio.2021.01.004
- Hobbs, S., Reynoso, M., Geddis, A. V., Mitrophanov, A. Y., & Matheny, R. W., Jr. (2018). LPS-stimulated NF-kappaB p65 dynamic response marks the initiation of TNF expression and transition to IL-10 expression in RAW 264.7 macrophages. *Physiol Rep*, 6(21), e13914. doi:10.14814/phy2.13914
- Hou, F., Sun, L., Zheng, H., Skaug, B., Jiang, Q. X., & Chen, Z. J. (2011). MAVS forms functional prion-like aggregates to activate and propagate antiviral innate immune response. *Cell*, 146(3), 448-461. doi:10.1016/j.cell.2011.06.041
- Howe, K., Clark, M. D., Torroja, C. F., Torrance, J., Berthelot, C., Muffato, M., . . . Stemple, D. L. (2013). The zebrafish reference genome sequence and its relationship to the human genome. *Nature*, 496(7446), 498-503. doi:10.1038/nature12111

- Iguchi, Y., Eid, L., Parent, M., Soucy, G., Bareil, C., Riku, Y., . . . Julien, J. P. (2016). Exosome secretion is a key pathway for clearance of pathological TDP-43. *Brain*, *139*(Pt 12), 3187-3201. doi:10.1093/brain/aww237
- Ingre, C., Roos, P. M., Piehl, F., Kamel, F., & Fang, F. (2015). Risk factors for amyotrophic lateral sclerosis. *Clin Epidemiol*, *7*, 181-193. doi:10.2147/CLEP.S37505
- Jimenez-Dalmaroni, M. J., Gerswhin, M. E., & Adamopoulos, I. E. (2016). The critical role of toll-like receptors--From microbial recognition to autoimmunity: A comprehensive review. *Autoimmun Rev*, *15*(1), 1-8. doi:10.1016/j.autrev.2015.08.009
- Jin, J., Xiao, Y., Chang, J. H., Yu, J., Hu, H., Starr, R., . . . Sun, S. C. (2012). The kinase TBK1 controls IgA class switching by negatively regulating noncanonical NF-kappaB signaling. *Nat Immunol*, *13*(11), 1101-1109. doi:10.1038/ni.2423
- Kawai, T., Takahashi, K., Sato, S., Coban, C., Kumar, H., Kato, H., . . . Akira, S. (2005). IPS-1, an adaptor triggering RIG-I- and Mda5-mediated type I interferon induction. *Nat Immunol*, *6*(10), 981-988. doi:10.1038/ni1243
- Kiernan, M. C., Vucic, S., Cheah, B. C., Turner, M. R., Eisen, A., Hardiman, O., . . . Zoing, M. C. (2011). Amyotrophic lateral sclerosis. *Lancet*, *377*(9769), 942-955. doi:10.1016/S0140-6736(10)61156-7
- Kurosaki, T., & Maquat, L. E. (2016). Nonsense-mediated mRNA decay in humans at a glance. *J Cell Sci*, *129*(3), 461-467. doi:10.1242/jcs.181008
- Kwiatkowski, T. J., Jr., Bosco, D. A., Leclerc, A. L., Tamrazian, E., Vanderburg, C. R., Russ, C., . . . Brown, R. H., Jr. (2009). Mutations in the FUS/TLS gene on chromosome 16 cause familial amyotrophic lateral sclerosis. *Science*, *323*(5918), 1205-1208. doi:10.1126/science.1166066
- Kwon, H. S., & Koh, S. H. (2020). Neuroinflammation in neurodegenerative disorders: the roles of microglia and astrocytes. *Transl Neurodegener*, *9*(1), 42. doi:10.1186/s40035-020-00221-2
- Lafont, E., Draber, P., Rieser, E., Reichert, M., Kupka, S., de Miguel, D., . . . Walczak, H. (2018). TBK1 and IKKepsilon prevent TNF-induced cell death by RIPK1 phosphorylation. *Nat Cell Biol*, *20*(12), 1389-1399. doi:10.1038/s41556-018-0229-6
- Larabi, A., Devos, J. M., Ng, S. L., Nanao, M. H., Round, A., Maniatis, T., & Panne, D. (2013). Crystal structure and mechanism of activation of TANK-binding kinase 1. *Cell Rep*, *3*(3), 734-746. doi:10.1016/j.celrep.2013.01.034
- Lazarou, M., Sliter, D. A., Kane, L. A., Sarraf, S. A., Wang, C., Burman, J. L., . . . Youle, R. J. (2015). The ubiquitin kinase PINK1 recruits autophagy receptors to induce mitophagy. *Nature*, *524*(7565), 309-314. doi:10.1038/nature14893
- Le Ber, I., De Septenville, A., Millecamps, S., Camuzat, A., Caroppo, P., Couratier, P., . . . Genetic Research Network on, F. F.-A. (2015). TBK1 mutation frequencies in French frontotemporal dementia and amyotrophic lateral sclerosis cohorts. *Neurobiol Aging*, *36*(11), 3116 e3115-3116 e3118. doi:10.1016/j.neurobiolaging.2015.08.009
- Ling, S. C., Polymenidou, M., & Cleveland, D. W. (2013). Converging mechanisms in ALS and FTD: disrupted RNA and protein homeostasis. *Neuron*, *79*(3), 416-438. doi:10.1016/j.neuron.2013.07.033
- Liu, J., & Wang, F. (2017). Role of Neuroinflammation in Amyotrophic Lateral Sclerosis: Cellular Mechanisms and Therapeutic Implications. *Front Immunol*, *8*, 1005. doi:10.3389/fimmu.2017.01005

- Liu, S., Cai, X., Wu, J., Cong, Q., Chen, X., Li, T., . . . Chen, Z. J. (2015). Phosphorylation of innate immune adaptor proteins MAVS, STING, and TRIF induces IRF3 activation. *Science*, *347*(6227), aaa2630. doi:10.1126/science.aaa2630
- Liu, Z., Cheng, X., Zhong, S., Zhang, X., Liu, C., Liu, F., & Zhao, C. (2020). Peripheral and Central Nervous System Immune Response Crosstalk in Amyotrophic Lateral Sclerosis. *Front Neurosci*, *14*, 575. doi:10.3389/fnins.2020.00575
- Longinetti, E., & Fang, F. (2019). Epidemiology of amyotrophic lateral sclerosis: an update of recent literature. *Curr Opin Neurol*, *32*(5), 771-776. doi:10.1097/WCO.0000000000000730
- Ma, X., Helgason, E., Phung, Q. T., Quan, C. L., Iyer, R. S., Lee, M. W., . . . Dueber, E. C. (2012). Molecular basis of Tank-binding kinase 1 activation by transautophosphorylation. *Proc Natl Acad Sci U S A*, *109*(24), 9378-9383. doi:10.1073/pnas.1121552109
- Marchlik, E., Thakker, P., Carlson, T., Jiang, Z., Ryan, M., Marusic, S., . . . Hall, J. P. (2010). Mice lacking Tbk1 activity exhibit immune cell infiltrates in multiple tissues and increased susceptibility to LPS-induced lethality. *J Leukoc Biol*, *88*(6), 1171-1180. doi:10.1189/jlb.0210071
- Masrori, P., & Van Damme, P. (2020). Amyotrophic lateral sclerosis: a clinical review. *Eur J Neurol*, *27*(10), 1918-1929. doi:10.1111/ene.14393
- Miller, R. G., Mitchell, J. D., & Moore, D. H. (2012). Riluzole for amyotrophic lateral sclerosis (ALS)/motor neuron disease (MND). *Cochrane Database Syst Rev*, *2012*(3), CD001447. doi:10.1002/14651858.CD001447.pub3
- Miller, T. M., Cudkowicz, M. E., Genge, A., Shaw, P. J., Sobue, G., Bucelli, R. C., . . . Group, O. L. E. W. (2022). Trial of Antisense Oligonucleotide Tofersen for SOD1 ALS. *N Engl J Med*, *387*(12), 1099-1110. doi:10.1056/NEJMoa2204705
- Mittal, S. K., & Roche, P. A. (2015). Suppression of antigen presentation by IL-10. *Curr Opin Immunol*, *34*, 22-27. doi:10.1016/j.coi.2014.12.009
- Moloney, E. B., de Winter, F., & Verhaagen, J. (2014). ALS as a distal axonopathy: molecular mechanisms affecting neuromuscular junction stability in the presymptomatic stages of the disease. *Front Neurosci*, *8*, 252. doi:10.3389/fnins.2014.00252
- Moore, A. S., & Holzbaur, E. L. (2016). Dynamic recruitment and activation of ALS-associated TBK1 with its target optineurin are required for efficient mitophagy. *Proc Natl Acad Sci U S A*, *113*(24), E3349-3358. doi:10.1073/pnas.1523810113
- Muzio, L., Viotti, A., & Martino, G. (2021). Microglia in Neuroinflammation and Neurodegeneration: From Understanding to Therapy. *Front Neurosci*, *15*, 742065. doi:10.3389/fnins.2021.742065
- Neupane, P., Thada, P. K., Singh, P., Faisal, A. R., Rai, N., Poudel, P., . . . Jain, E. (2023). Investigating Edaravone Use for Management of Amyotrophic Lateral Sclerosis (ALS): A Narrative Review. *Cureus*, *15*(1), e33746. doi:10.7759/cureus.33746
- Novoa, B., Bowman, T. V., Zon, L., & Figueras, A. (2009). LPS response and tolerance in the zebrafish (*Danio rerio*). *Fish Shellfish Immunol*, *26*(2), 326-331. doi:10.1016/j.fsi.2008.12.004
- Oakes, J. A., Davies, M. C., & Collins, M. O. (2017). TBK1: a new player in ALS linking autophagy and neuroinflammation. *Mol Brain*, *10*(1), 5. doi:10.1186/s13041-017-0287-x
- Orsini, M., Oliveira, A. B., Nascimento, O. J., Reis, C. H., Leite, M. A., de Souza, J. A., . . . Smidt, B. (2015). Amyotrophic Lateral Sclerosis: New Perspectives and Update. *Neurol Int*, *7*(2), 5885. doi:10.4081/ni.2015.5885

- Oskarsson, B., Gendron, T. F., & Staff, N. P. (2018). Amyotrophic Lateral Sclerosis: An Update for 2018. *Mayo Clin Proc*, *93*(11), 1617-1628. doi:10.1016/j.mayocp.2018.04.007
- Oskarsson, B., Horton, D. K., & Mitsumoto, H. (2015). Potential Environmental Factors in Amyotrophic Lateral Sclerosis. *Neurol Clin*, *33*(4), 877-888. doi:10.1016/j.ncl.2015.07.009
- Paganoni, S., Hendrix, S., Dickson, S. P., Knowlton, N., Berry, J. D., Elliott, M. A., . . . Cudkowicz, M. (2022). Effect of sodium phenylbutyrate/taurursodiol on tracheostomy/ventilation-free survival and hospitalisation in amyotrophic lateral sclerosis: long-term results from the CENTAUR trial. *J Neurol Neurosurg Psychiatry*, *93*(8), 871-875. doi:10.1136/jnnp-2022-329024
- Peters, O. M., Ghasemi, M., & Brown, R. H., Jr. (2015). Emerging mechanisms of molecular pathology in ALS. *J Clin Invest*, *125*(6), 2548. doi:10.1172/JCI82693
- Power, M. R., Peng, Y., Maydanski, E., Marshall, J. S., & Lin, T. J. (2004). The development of early host response to *Pseudomonas aeruginosa* lung infection is critically dependent on myeloid differentiation factor 88 in mice. *J Biol Chem*, *279*(47), 49315-49322. doi:10.1074/jbc.M402111200
- Ragagnin, A. M. G., Shadfar, S., Vidal, M., Jamali, M. S., & Atkin, J. D. (2019). Motor Neuron Susceptibility in ALS/FTD. *Front Neurosci*, *13*, 532. doi:10.3389/fnins.2019.00532
- Reis, J., Guan, X. Q., Kisselev, A. F., Papasian, C. J., Qureshi, A. A., Morrison, D. C., . . . Qureshi, N. (2011). LPS-induced formation of immunoproteasomes: TNF-alpha and nitric oxide production are regulated by altered composition of proteasome-active sites. *Cell Biochem Biophys*, *60*(1-2), 77-88. doi:10.1007/s12013-011-9182-8
- Renton, A. E., Majounie, E., Waite, A., Simon-Sanchez, J., Rollinson, S., Gibbs, J. R., . . . Traynor, B. J. (2011). A hexanucleotide repeat expansion in C9ORF72 is the cause of chromosome 9p21-linked ALS-FTD. *Neuron*, *72*(2), 257-268. doi:10.1016/j.neuron.2011.09.010
- Rosen, D. R., Siddique, T., Patterson, D., Figlewicz, D. A., Sapp, P., Hentati, A., . . . et al. (1993). Mutations in Cu/Zn superoxide dismutase gene are associated with familial amyotrophic lateral sclerosis. *Nature*, *362*(6415), 59-62. doi:10.1038/362059a0
- Roussel, Y., Gaudreau, S. F., Kacer, E. R., Sengupta, M., & Bui, T. V. (2021). Modeling spinal locomotor circuits for movements in developing zebrafish. *Elife*, *10*. doi:10.7554/eLife.67453
- Rowland, L. P. (2001). How amyotrophic lateral sclerosis got its name: the clinical-pathologic genius of Jean-Martin Charcot. *Arch Neurol*, *58*(3), 512-515. doi:10.1001/archneur.58.3.512
- Runde, A. P., Mack, R., S, J. P., & Zhang, J. (2022). The role of TBK1 in cancer pathogenesis and anticancer immunity. *J Exp Clin Cancer Res*, *41*(1), 135. doi:10.1186/s13046-022-02352-y
- Rutherford, N. J., Zhang, Y. J., Baker, M., Gass, J. M., Finch, N. A., Xu, Y. F., . . . Rademakers, R. (2008). Novel mutations in TARDBP (TDP-43) in patients with familial amyotrophic lateral sclerosis. *PLoS Genet*, *4*(9), e1000193. doi:10.1371/journal.pgen.1000193
- Saint-Amant, L., & Drapeau, P. (2000). Motoneuron activity patterns related to the earliest behavior of the zebrafish embryo. *J Neurosci*, *20*(11), 3964-3972. doi:10.1523/JNEUROSCI.20-11-03964.2000

- Scotter, E. L., Chen, H. J., & Shaw, C. E. (2015). TDP-43 Proteinopathy and ALS: Insights into Disease Mechanisms and Therapeutic Targets. *Neurotherapeutics*, *12*(2), 352-363. doi:10.1007/s13311-015-0338-x
- Seth, R. B., Sun, L., Ea, C. K., & Chen, Z. J. (2005). Identification and characterization of MAVS, a mitochondrial antiviral signaling protein that activates NF-kappaB and IRF 3. *Cell*, *122*(5), 669-682. doi:10.1016/j.cell.2005.08.012
- Sieverding, K., Ulmer, J., Bruno, C., Satoh, T., Tsao, W., Freischmidt, A., . . . Weishaupt, J. H. (2021). Hemizygous deletion of Tbk1 worsens neuromuscular junction pathology in TDP-43(G298S) transgenic mice. *Exp Neurol*, *335*, 113496. doi:10.1016/j.expneurol.2020.113496
- Smeyers, J., Banchi, E. G., & Latouche, M. (2021). C9ORF72: What It Is, What It Does, and Why It Matters. *Front Cell Neurosci*, *15*, 661447. doi:10.3389/fncel.2021.661447
- Smith, E. F., Shaw, P. J., & De Vos, K. J. (2019). The role of mitochondria in amyotrophic lateral sclerosis. *Neurosci Lett*, *710*, 132933. doi:10.1016/j.neulet.2017.06.052
- Smith, H., Liu, X. Y., Dai, L., Goh, E. T., Chan, A. T., Xi, J., . . . Cheung, P. C. (2011). The role of TBK1 and IKKepsilon in the expression and activation of Pellino 1. *Biochem J*, *434*(3), 537-548. doi:10.1042/BJ20101421
- Talbot, E. O., Malek, A. M., & Lacomis, D. (2016). The epidemiology of amyotrophic lateral sclerosis. *Handb Clin Neurol*, *138*, 225-238. doi:10.1016/B978-0-12-802973-2.00013-6
- Tojima, Y., Fujimoto, A., Delhase, M., Chen, Y., Hatakeyama, S., Nakayama, K., . . . Nakanishi, M. (2000). NAK is an IkappaB kinase-activating kinase. *Nature*, *404*(6779), 778-782. doi:10.1038/35008109
- Valencia, M., Kim, S. R., Jang, Y., & Lee, S. H. (2021). Neuronal Autophagy: Characteristic Features and Roles in Neuronal Pathophysiology. *Biomol Ther (Seoul)*, *29*(6), 605-614. doi:10.4062/biomolther.2021.012
- Van Den Bosch, L., Van Damme, P., Bogaert, E., & Robberecht, W. (2006). The role of excitotoxicity in the pathogenesis of amyotrophic lateral sclerosis. *Biochim Biophys Acta*, *1762*(11-12), 1068-1082. doi:10.1016/j.bbadis.2006.05.002
- Vance, C., Rogelj, B., Hortobagyi, T., De Vos, K. J., Nishimura, A. L., Sreedharan, J., . . . Shaw, C. E. (2009). Mutations in FUS, an RNA processing protein, cause familial amyotrophic lateral sclerosis type 6. *Science*, *323*(5918), 1208-1211. doi:10.1126/science.1165942
- Vargas, J. N. S., Wang, C., Bunker, E., Hao, L., Maric, D., Schiavo, G., . . . Youle, R. J. (2019). Spatiotemporal Control of ULK1 Activation by NDP52 and TBK1 during Selective Autophagy. *Mol Cell*, *74*(2), 347-362 e346. doi:10.1016/j.molcel.2019.02.010
- Wang, H., Guan, L., & Deng, M. (2023). Recent progress of the genetics of amyotrophic lateral sclerosis and challenges of gene therapy. *Front Neurosci*, *17*, 1170996. doi:10.3389/fnins.2023.1170996
- Weidberg, H., & Elazar, Z. (2011). TBK1 mediates crosstalk between the innate immune response and autophagy. *Sci Signal*, *4*(187), pe39. doi:10.1126/scisignal.2002355
- Wu, J., Sun, L., Chen, X., Du, F., Shi, H., Chen, C., & Chen, Z. J. (2013). Cyclic GMP-AMP is an endogenous second messenger in innate immune signaling by cytosolic DNA. *Science*, *339*(6121), 826-830. doi:10.1126/science.1229963
- Xie, Y., Meijer, A. H., & Schaaf, M. J. M. (2020). Modeling Inflammation in Zebrafish for the Development of Anti-inflammatory Drugs. *Front Cell Dev Biol*, *8*, 620984. doi:10.3389/fcell.2020.620984

- Xu, D., Jin, T., Zhu, H., Chen, H., Ofengeim, D., Zou, C., . . . Yuan, J. (2018). TBK1 Suppresses RIPK1-Driven Apoptosis and Inflammation during Development and in Aging. *Cell*, *174*(6), 1477-1491 e1419. doi:10.1016/j.cell.2018.07.041
- Xu, L., Chen, L., Wang, S., Feng, J., Liu, L., Liu, G., . . . Fan, D. (2020). Incidence and prevalence of amyotrophic lateral sclerosis in urban China: a national population-based study. *J Neurol Neurosurg Psychiatry*, *91*(5), 520-525. doi:10.1136/jnnp-2019-322317
- Yu, T., Yi, Y. S., Yang, Y., Oh, J., Jeong, D., & Cho, J. Y. (2012). The pivotal role of TBK1 in inflammatory responses mediated by macrophages. *Mediators Inflamm*, *2012*, 979105. doi:10.1155/2012/979105
- Zarei, S., Carr, K., Reiley, L., Diaz, K., Guerra, O., Altamirano, P. F., . . . Chinea, A. (2015). A comprehensive review of amyotrophic lateral sclerosis. *Surg Neurol Int*, *6*, 171. doi:10.4103/2152-7806.169561
- Zhao, B., Du, F., Xu, P., Shu, C., Sankaran, B., Bell, S. L., . . . Li, P. (2019). A conserved PLPLRT/SD motif of STING mediates the recruitment and activation of TBK1. *Nature*, *569*(7758), 718-722. doi:10.1038/s41586-019-1228-x
- Zhou, R., Zhang, Q., & Xu, P. (2020). TBK1, a central kinase in innate immune sensing of nucleic acids and beyond. *Acta Biochim Biophys Sin (Shanghai)*, *52*(7), 757-767. doi:10.1093/abbs/gmaa051